Supporting Information

Identification of Cryptic Products of the Gliotoxin Gene Cluster Using NMR-Based Comparative Metabolomics and a Model for Gliotoxin Biosynthesis

Ry R. Forseth,[†] Ellen M. Fox,[‡] DaWoon Chung,[§] Barbara J. Howlett,[‡] Nancy P. Keller,[§] Frank C. Schroeder[†]

[†]Boyce Thompson Institute and Department of Chemistry and Chemical Biology, Cornell University, Ithaca, New York 14853; United States

[‡]School of Botany, The University of Melbourne, Victoria, 3010, Australia

[§]Department of Medical Microbiology and Immunology, University of Wisconsin-Madison, Madison, Wisconsin 53706, United States

Contents

Methods

1. General Analytical Methods and Equipment. (a) NMR Spectroscopy, NMR spectroscopic instrumentation: a Varian INOVA 600 MHz NMR spectrometer (600.0 MHz ^{1}H reference frequency, 150.6 MHz for ^{13}C) equipped with an HCN indirect-detection probe, a Varian 900 MHz NMR spectrometer (899.9 MHz ^{1}H reference frequency, 226.7 MHz for ^{13}C) equipped with a 5 mm ^{1}H{^{13}C/^{15}N} Cryogenic Probe, and a Bruker AVANCE 600 MHz NMR spectrometer (600.7 MHz ^{1}H reference frequency, 149.9 MHz for ^{13}C) equipped with a 5 mm TXI probe. Non-gradient phase-cycled dqfCOSY spectra were acquired using the following parameters: 0.6 s acquisition time, 500-900 complex increments, 8-32 scans per increment. ROESY spectra were acquired using the following parameters: 0.25 s acquisition time, 0.2-0.4 s mixing time, 200-400 increments, 16-32 scans per increment. Gradient and non-gradient HSQC[AD], HMQC, and HMBC[AD] spectra were acquired with these parameters: 0.25 s acquisition time, 300-600 increments, 4-32 scans per increment. ^{1}H,^{13}C-HMBC spectra were optimized for $J_{H,C}$ = 6 Hz. ^{1}H,^{15}N-gHMBCAD spectra were optimized for $J_{H,15N}$ = 8 Hz. Susceptibility-matched NMR tubes (Shigemi) were used for sample amounts smaller than 2 mg. NMR spectra were processed and baseline corrected using Varian VNMR and MestreLabs MestReC and MNOVA software packages. **(b) Mass spectrometry**, High-resolution mass spectrometry was performed on a LTQ Orbitrap Velos (Thermo Scientific) or a SYNAPT HDMS: (Q-IMS-TOF). HPLC system equipped with a diode array detector and connected to a Quattro II spectrometer (Micromass/Waters) operated in positive-ion electrospray ionization (ESI^{+}) mode was used for HPLC-MS analysis. Data acquisition and processing for the HPLC-MS was controlled by Waters MassLynx software. **(c) Chromatography**, Flash chromatography was performed using a Teledyne ISCO CombiFlash system. For semi-preparative HPLC Supelco Discovery HS C-18 column (25 cm x 10 mm, 5 µm particle diameter). An Agilent Zorbax Eclipse XDB-C8 column (4.6 x 150 mm, 5 µm particle diameter) was used in HPLC-MS analysis.

2. Fungal Strains and Experimental Growth Conditions. *Aspergillus fumigatus* strains: AF293 (wild type), TDWC5.6 (∆gliZ:: *A. parasiticus pyrG*; *pyrG1*), ARC2 (∆*gliP::A*. *parasiticus pyrG pyrG1)* donated by William J. Steinbach; Duke University, *⊿gliI* (*gliI:A. parasiticus pyrG; pyrG1*). Strains were maintained as glycerol stocks and were cultured at 25°C on glucose minimal medium (GMM).[1]

For preparation of spore suspensions, two week old cultures of WT, OE, ∆*gliZ*, ∆*gliP*, and ∆*gliI*, grown on GMM plates, were flooded with 1 ml 0.01% Tween 20. 100 µL of the fluid from the

flooded plates was diluted with 0.8 mL 0.01% Tween 20 to make the spore suspensions for inoculation. 7 µl of the spore suspension was point inoculated onto the middle of GMM plates. For initial and replicate studies of WT, Δ*gliZ*, and Δ*gliI* twenty plates of each strain were cultured. For DANS comparison studies of OE to WT, and Δ*gliZ*, three GMM plates of each strain were grown. Cultures were grown for two weeks at 25 °C in the dark. Culturing procedures for Δ*gliP* are described below in section 13.

3. Construction of *gliI* Knock Out Mutants (Δ*gliI*). To delete *gliI* in *A. fumigatus*, the plasmid pDWC8.5 was designed as follows. A PCR amplicon of 898 bp of the *gliI* upstream sequence was digested using *SalI* and *EcoRI*, and ligated into *SalI-EcoRI* digested pJW24 vector carrying *A. parasiticus pyrG*. The resulting vector was digested using *BamHI* and *NotI* and ligated with a *BamHI-NotI* digested PCR amplicon of 889 bp of the *gliI* downstream sequence. This final vector was designated as pDWC8.5. To generate the Δ*gliI* strain (TDWC7.49 and TDWC7.54), DNA of pDWC8.5 was transformed into *A. fumigatus* wild type AF293.1. Homologous recombination of the *gliI* knock-out construct was verified by PCR and Southern blot analysis (Figure S4).

4. Assesment of *gliZ* and *gliP* Expression in Δ*gliI* Mutant. Northern analysis was used to assess gene expression in *A. fumigatus* strains. Total RNA was extracted from lyophilized mycelia of *A. fumigatus* using TRIzol (Invitrogen) and separated on a denaturing formaldehyde/agarose gel. RNA was transferred from the gel to a nylon membrane (Hybond^{TM}-N^{+}, Amersham Pharmacia Biotech) by capillary blotting with 10 x SSC. RNA was irreversibly bound to the membrane using a UV cross linker at 1200 J^{3}cm^{-2}. Blots of *A. fumigatus* RNA were hybridized with the following fragments, which had been amplified from *A. fumigatus* genomic DNA and labeled with [^{32}P] αdCTP: a 653 bp fragment of *gliI* (primers 5'-TGTTGATCGAGACGCCGTTCTG-3' and 5'-CAGAGCGGCTCGATTCTGGTG-3'), a 1211 bp fragment of *gliZ* (primers 5'-AAGGGCCGGTAGTCTACCTCTTC-3' and 5'-CGATCTGGTAGCTGCCCAGCTGGAAG-3') and a 173 bp fragment of *gliP* (primers 5'-AAACCCCTGTGAATGCAGAC-3' and 5'-CCCCTTGAGATGAAAGGTGA-3') (Figure S5).

5. Metabolome Extraction and Initial Fractionation. Fungal cultures including fungal tissue and agar media were cut into small ~1 x 1 cm cubes and placed into individual 1 L round bottom flasks, frozen using a dry ice acetone bath, and lyophilized. Two different protocols were used for extraction of fungal cultures: (1) lyophilized WT and Δ*gliZ* cultures were extracted with ethyl acetate and a mixture of 5% ethyl acetate, 15% water, and 80% acetonitrile; (2) for additional

analysis of WT and Δ*gliZ* cultures and for analyses of the Δ*gliP* and Δ*gliI* cultures 100% ethyl acetate followed by 100% acetonitrile were used to extract the lyophilized fungal cultures. All extracts were filtered over Celite and a glass frit. Subsequently, the extracts were adsorbed onto Celite (~1 g of Celite for 100 mg of dried extract) and fractionated on a 100 g RediSep Reverse-Phase (RP) C-18 flash chromatography column using a water-acetonitrile solvent gradient, starting with 20 min of 5% acetonitrile followed by a linear increase to 100% acetonitrile over 40 min, followed by 10 min of 100% acetonitrile. Fractions were combined into three pools; pool 1, 0.5% acetonitrile isocratic elution, fractions 21-44; pool 2, 0.5-55% acetonitrile, fractions 45–101; pool 3, 55-100% acetonitrile, fractions 102-140. Pools were evaporated to dryness and suspended in ~0.2 mL of acetonitrile-d_3 (in the case of pool 1, ~0.2 mL 1:2 D_2O:acetonitrile-d_3). The suspension was centrifuged to remove insoluble materials; this was repeated two additional times, and the supernatant was subjected to NMR spectroscopic analysis.

6. Differential Analysis by 2D-NMR Spectroscopy (adapted from reference[2]). High-resolution dqfCOSY spectra were acquired using the following parameters: acquisition time 0.6 s; 500 increments (ni). Phase cycling was used for coherence selection, and MestReC was used to process the resulting data, zero-filling the spectra to 8096 complex data points in the directly detected dimension (F2) and 4096 data points in the indirectly detected dimension (F1). Bitmaps derived from absolute-value processed dqfCOSY spectra were then imported into Adobe Photoshop CS3 and overlayed as described in reference[3].

7. Characterization of Compounds 10-14a/b, 16, and 17. The WT-derived pools used for DANS analysis described above was fractionated using a Supelco Discovery HS C-18 column (25 cm x 10 mm, 5 µm particle diameter) and a water-acetonitrile solvent gradient, starting with 5 min at 5% acetonitrile, followed by a linear increase to 23% acetonitrile over 1 min, and a more gradual increase reaching 50% acetonitrile at 49 min. A total of 18 fractions were collected. Fractions 1-18 were evaporated to dryness *in vacuo* and dissolved in acetonitrile-d_3, followed by ^{1}H-NMR spectroscopic analysis of each fraction. Comparison with data from DANS analyses indicated that fraction 1 contained nearly pure compound **10**, and fraction 5 contained nearly pure compound **11**. Comparison with the DANS data further indicated that compounds **12**, **14b**, and **16** were present in fraction 2, and compounds **13**, **14a**, and **17** in fraction 4.

Fractions 2 and 4 were further purified using the same column and solvent system described above. Fraction 2 was separated to obtain samples of **12**, **14b**, and **16** using a solvent gradient starting at 5% acetonitrile for 30 min, followed by a linear increase to 20 % acetonitrile over 30

min, which was followed by 10 min at 20% acetonitrile. Fraction 4 was fractionated further to obtain samples of **13**, **14a**, and **17** using a solvent gradient of 30 min at 5% acetonitrile with a linear increase to 20 % over 5 min followed by 12 min 20% acetonitrile. In each case collected fractions were evaporated to dryness *in vacuo* and dissolved in acetonitrile-d_3, followed by NMR spectroscopic analysis of each fraction.

8. Purification of Compound 4. 20 WT cultures grown on GMM plates, as described above, were extracted using a mixture of 5% ethyl acetate, 15% water, and 80% acetonitrile (section 2). These extracts were initially used to determine an appropriate enrichment protocol for compound **4**. WT extracts were dissolved in ~50 % acetonitrile/water and absorbed onto Celite. Solvent was removed *in vacuo*. The sample, absorbed onto Celite, was subjected to flash chromatography using a CombiFlash chromatography system equipped with a 100 g RediSep Gold RP-18 flash chromatography column using acetonitrile and 0.1% acetic acid in water as solvents, starting with 3.5 min at 1% acetonitrile, followed by a linear increase to 10% acetonitrile over 16 min, which was followed by an increase to 100% acetonitrile over 3.5 min, holding at 100% acetonitrile for 3.5 min. Fractions were evaporated to dryness, and ^{1}H NMR spectra of individual fractions were acquired in methanol-d_4. Signals diagnostic for compound **4**, including signals representing olefinic, methylene, and methyl sulfanyl protons, indicated that **4** elutes at ~9% acetonitrile under these conditions. Fractions containing **4** were pooled together. For purification of a larger amount of compound **4**, this procedure described above was repeated twice more using extracts from two 90-plate-batches of WT. Fractions containing **4** were pooled to give a single sample of enriched **4** which was subjected further 2D NMR spectroscopic and HR-MS analysis.

9. Isolation of Compounds 15a/b. The remaining extract from the 200 WT cultures used for isolation of compound **4** was adsorbed onto Celite and subjected to flash chromatography using a CombiFlash chromatography system equipped with a 100 g RediSep Gold RP-18 column. The water-acetonitrile solvent gradient used is described in section 5 of the experimental procedures. Fractions eluting at 10-50% acetonitrile were pooled and evaporated *in vacuo*. The residue was dissolved in acetonitrile, filtered over acetonitrile-washed cotton, and subjected to preparative HPLC using instrumental setup and solvent systems described in section 6 of the experimental procedures. A water-acetonitrile solvent gradient was used that started at 5% acetonitrile for 30 min, followed by a linear increase to 20% acetonitrile over 30 min. (Compounds **15a/b** were found to elute at 13-14% acetonitrile under these conditions) Solvent was removed from the HPLC fractions *in vacuo* and samples were redissolved in acetonitrile-d_3,

and ^{1}H NMR spectra were acquired for each HPLC fraction. Diagnostic signals present in the DANS spectrum of pool 2 indicated the presence of **15a/b**.

10. High Resolution Mass Spectrometric Analysis for Compounds 4, 5-7, 9, 12, and 13-17. Enriched samples of compound **4**, **5**, **7**, **9**, and **15a/b** were diluted to 0.01 mg/mL by dissolving the samples in either 20% acetonitrile and 80% of 0.1% formic acid in water, **4**; or 50% acetonitrile and 50% of 0.1% formic acid in water, **5**-**7**, **9** and **15a/b**. These sample were infused into a LTQ Orbitrap Velos mass spectrometer running in ESI^+ ionization mode with a mass range at or within 1–2000 m/z.

Compound	HR-ESI^+MS Observed (m/z)	Ion	Calculated for Ion Formula	Calculated m/z
4	351.0434	$[M+Na]^+$	$C_{13}H_{16}N_2NaO_4S_2$	351.0438
5	325.0321	$[M+H]^+$	$C_{13}H_{13}N_2O_4S_2$	325.0311
6	357.0039	$[M+H]^+$	$C_{13}H_{13}N_2O_4S_3$	357.0032
7	388.9760	$[M+H]^+$	$C_{13}H_{13}N_2O_4S_4$	388.9753
9	377.0601	$[M+Na]^+$	$C_{15}H_{18}N_2NaO_4S_2$	377.0600
15a/b	317.0564	$[M+Na]^+$	$C_{13}H_{14}N_2NaO_4S$	317.0566

Samples of compounds **12**, **13**, **14a/b**, **16**, and **17** were diluted to a concentration 0.01 mg/mL in acetonitrile. An aliquot of the diluted sample was acidified using formic acid (final concentration 0.1%). Samples **12**, **13**, **14a/b**, **16**, and **17** were infused into a SYNAPT HDMS: (Q-IMS-TOF). Mass spectra were acquired using ESI^+ ionization with a mass range of 1-1000 m/z.

Compound	HR-ESI^+MS Observed (m/z)	Ion	Calculated for Ion Formula	Calculated m/z
12	281.107	$[M+H]^+$	$C_{13}H_{17}N_2O_3S$	281.095
13	365.055	$[M+Na]^+$	$C_{14}H_{18}N_2NaO_4S_2$	365.060
14a/b	333.106	$[M+Na]^+$	$C_{14}H_{18}N_2NaO_4S$	333.088
16	303.087	$[M+Na]^+$	$C_{13}H_{16}N_2NaO_5$	303.095
17	261.079	$[M+H]^+$	$C_{13}H_{13}N_2O_4$	261.087

11. HPLC-MS-based Comparison of WT and Mutant Extracts. Unfractionated WT and mutant extracts prepared as described in section 2 were dissolved in acetonitrile (~1 mL solvent/10 mg sample). Post-HPLC (using the RP-8 column) and UV spectroscopic analysis

(200-400 nm), samples were infused into a Quattro II ESI MS running in ESI^+ mode. Enriched samples of NMR- and MS-characterized *gliZ*-dependent metabolites served as elution time and ionization standards. Testing for the presence of compounds **1**-**3**, **8**, **10**-**12**, **14a**/**b**, and **17** in WT and mutant extracts a water/acetonitrile gradient was used starting with 5 min at 5% acetonitrile followed by a linear increase to 20% acetonitrile over 5 min, this was followed by a linear increase to 45% acetonitrile over 110 min (for chromatograms, see Figure S2 and S3). For testing the presence or absence of compounds **13** and **16** in WT and Δ*gliZ* extracts a different water/acetonitrile gradient was used starting with 5 min at 5% acetonitrile followed by a linear increase to 25% acetonitrile over 55 min.

12. Relative abundance of *gliZ*-dependent compounds. Using NMR solvent signals as internal standards, relative abundances of compounds **1**-**17** were estimated based on integration of their ^{1}H NMR spectroscopic signals in partially purified samples derived from a set of 20 WT plates. Abundance of *gliZ*-dependent metabolites relative to that of gliotoxin (**1**): compound **4**, 30:1; compound **10**, 2:1; compound **12**, 4:1; compound **11**, 8:1; compound **13**, 8:1; compound **14a**, 20:1; compound **14b**, 60:1; compound **16**, 50:1; compound **17**, 10:1, and compounds **2**, **3** and **8** ~1:1**.** Abundance of compounds **4** and **16** are likely underestimated significantly because of partial decomposition of these compounds during purification.

13. DANS of Δ*gliP* and WT. GMM plates were prepared as described in section 2, except that an additional 200 µL of sterile filtered (0.2 µm, pore size, Nalgene sterile filter) deionized water was pipetted onto the GMM plates prior to inoculation. For these studies sets of five GMM plates of each Δ*gliP* and WT were used. Plates were point inoculated, incubated, and extracted as described in above (sections 2 and 5).

14. Δ*gliP* Feeding Experiment. In parallel to the WT and Δ*gliP* cultures described above, five plates of Δ*gliP* supplied with synthetic compound **10** ("Δ*gliP*+***10***") were grown. For these cultures, 13 mg of **10**, purchased from Sigma-Aldrich, was dissolved in 3 mL deionized water and sterile filtered. 200 µL of this solution was pipetted onto each plate. Subsequently, plates were inoculated, incubated, and extracted as described above (Methods, sections 2 and 5). DANS comparison as well as HPLC-MS analysis of extracts derived from WT (positive control), Δ*gliP* (negative control), and Δ*gliP*+***10*** (treatment) revealed that none of the *gliZ*-dependent metabolites were rescued by addition of **10** to Δ*gliP*.

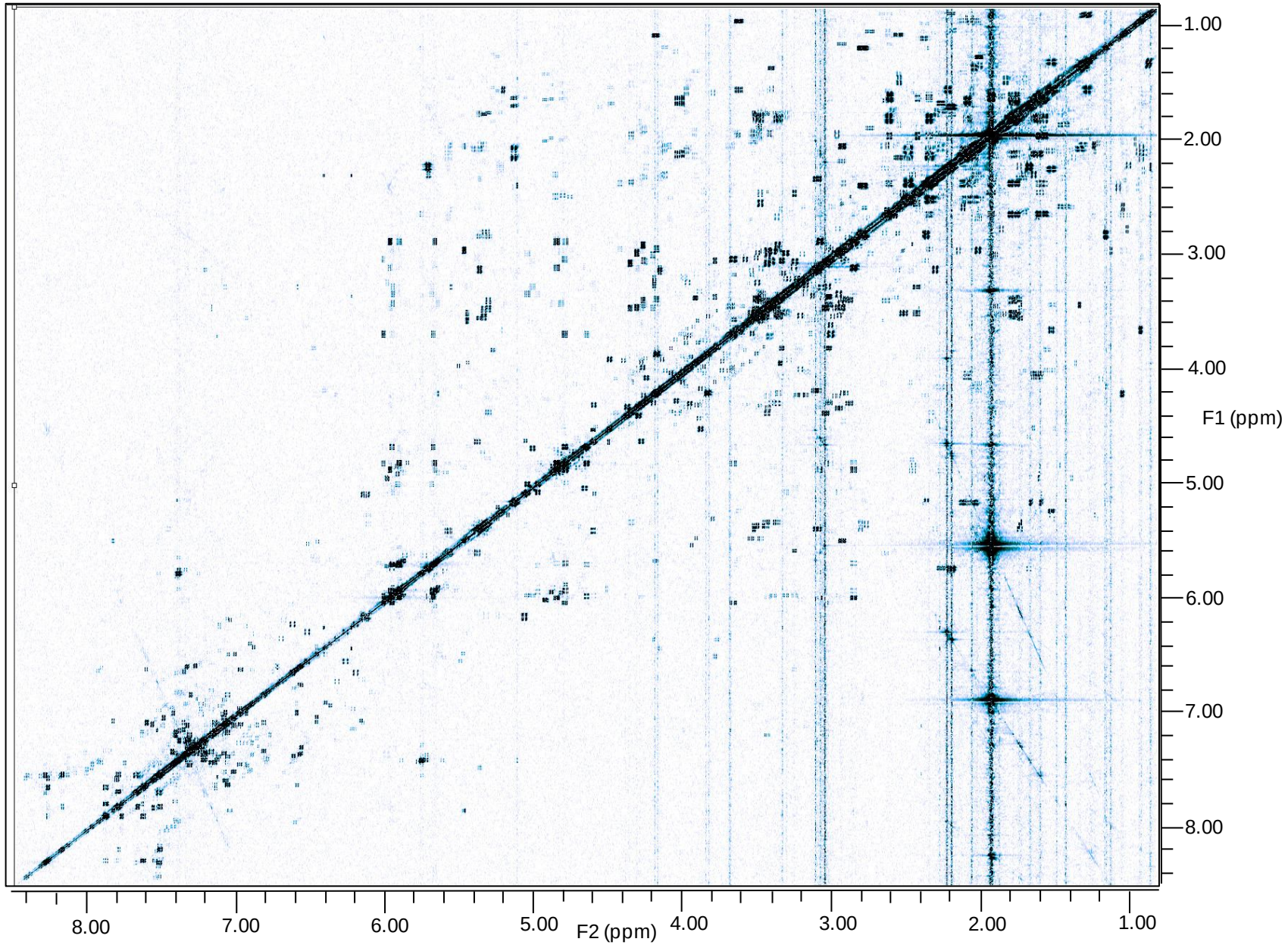

Figure S1A. Magnitude-mode processed dqfCOSY spectrum of *A. fumigatus* WT (600 MHz, solvent acetonitrile-d_3)

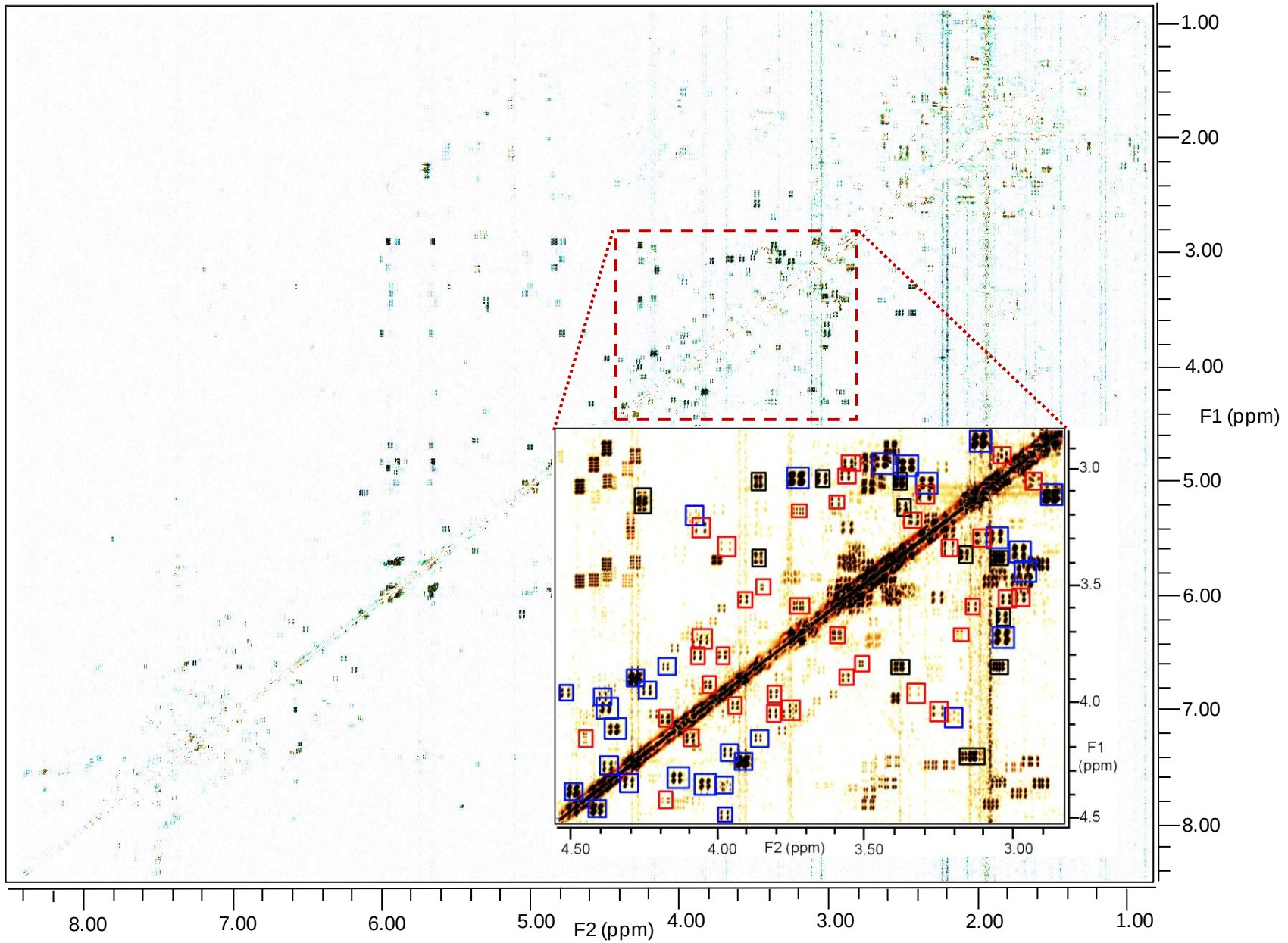

Figure S1B. DANS overlay of WT pool 2 and Δ*gliZ* pool 2, based on magnitude-mode processed dqfCOSY spectra (600 MHz, acetonitrile-d_3). Insert: 4.55-2.75 ppm section enhanced to reveal minor components. *gliZ*-dependent signals detected via DANS are boxed, representing known gliotoxin derivatives (blue), the known **10** and **11** (black), and novel compounds **12**-**17** (red).

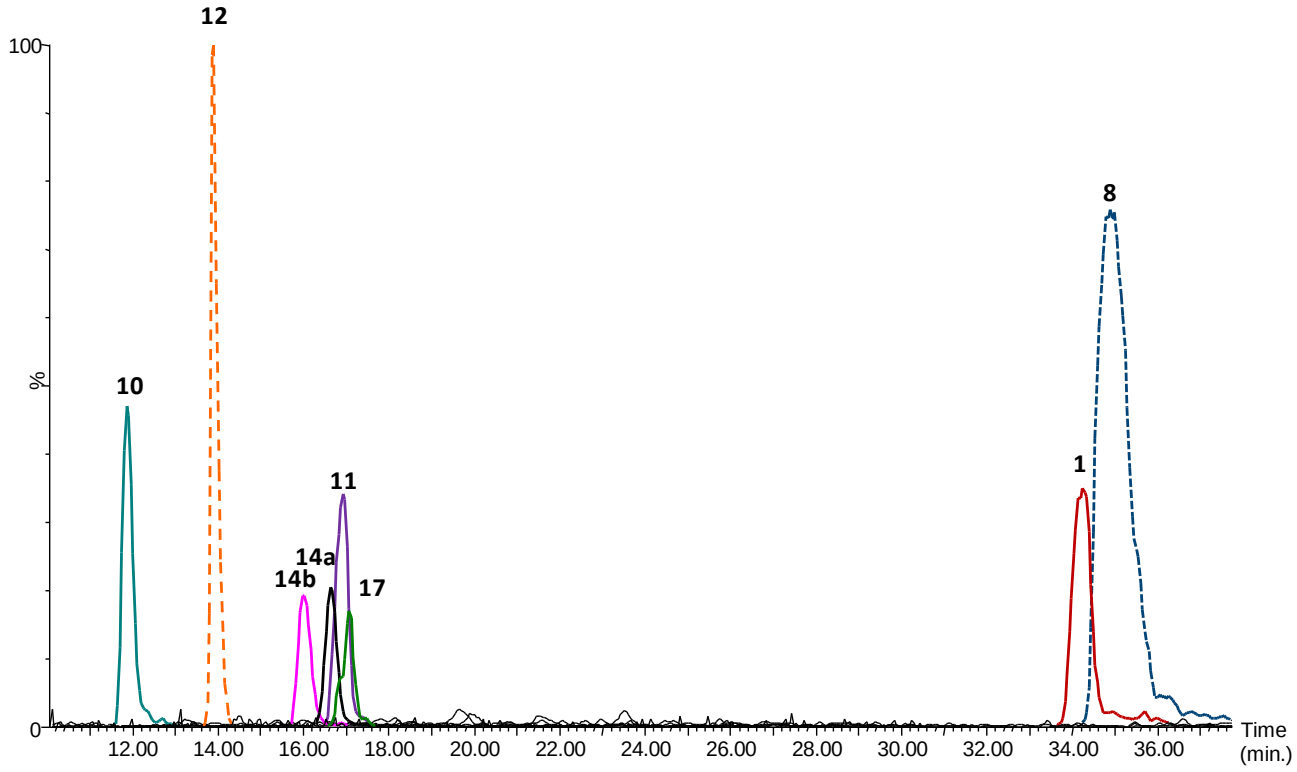

Figure S2. ESI$^+$MS ion chromatograms for *gliZ*-dependent metabolites **1**, **8**, **10**, **11**, **12**, **14a**, **14b**, and **17** obtained via HPLC-MS analysis of partially purified samples derived from *A. fumigatus* WT cultures. For each compound, a chromatogram representing the most abundantly produced ion is shown: m/z compound **1**, $[M\text{-}S_2+H]^+$ = 263.1; compound **10**, [M+1] = 235.1; compound **12**, $[M\text{-}SMe]^+$ = 233.1; compound **11**, $[M\text{-}SMe]^+$ = 279.1; compound **14a**, $[M\text{-}SMe]^+$ = 263.1; compound **14b**, $[M\text{-}SMe]^+$ = 263.1; compound **17**, $[M+H]^+$ = 261.1; and compound **8**, $[M+H]^+$ = 357.1.

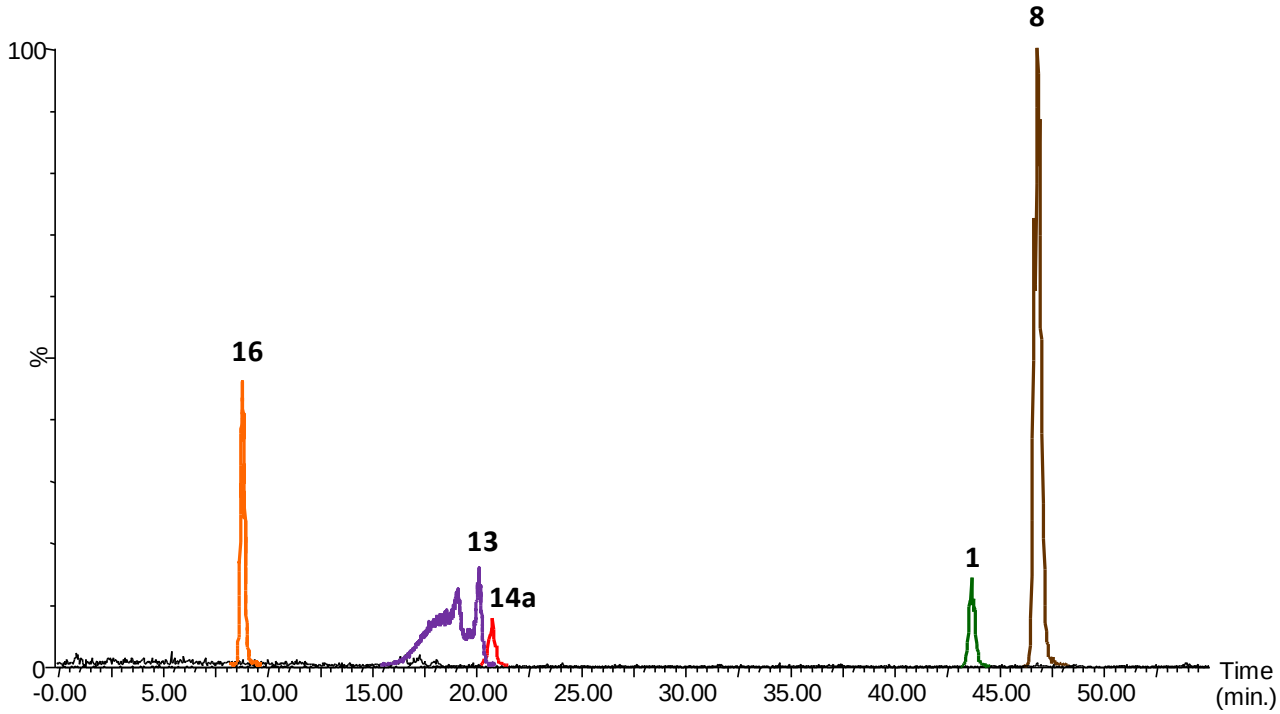

Figure S3. ESI$^+$MS ion chromatograms for *gliZ*-dependent metabolites **1**, **8**, **13**, **14a**, and **16** obtained via HPLC-MS analysis of partially purified samples derived from *A. fumigatus* WT cultures. Chromatograms for compounds **13** and **16** were obtained using single-ion recording MS. For each compound, a chromatogram representing the most abundantly produced ion is shown: m/z compound **16**, [M+1] = 281.1; compound **13**, $[M\text{-}SMe]^+$ = 295.1; compound **14a**, $[M\text{-}SMe]^+$ = 263.1; compound **1**, $[M\text{-}S_2+H]^+$ = 263.1; and compound **8**, $[M+H]^+$ = 357.1.

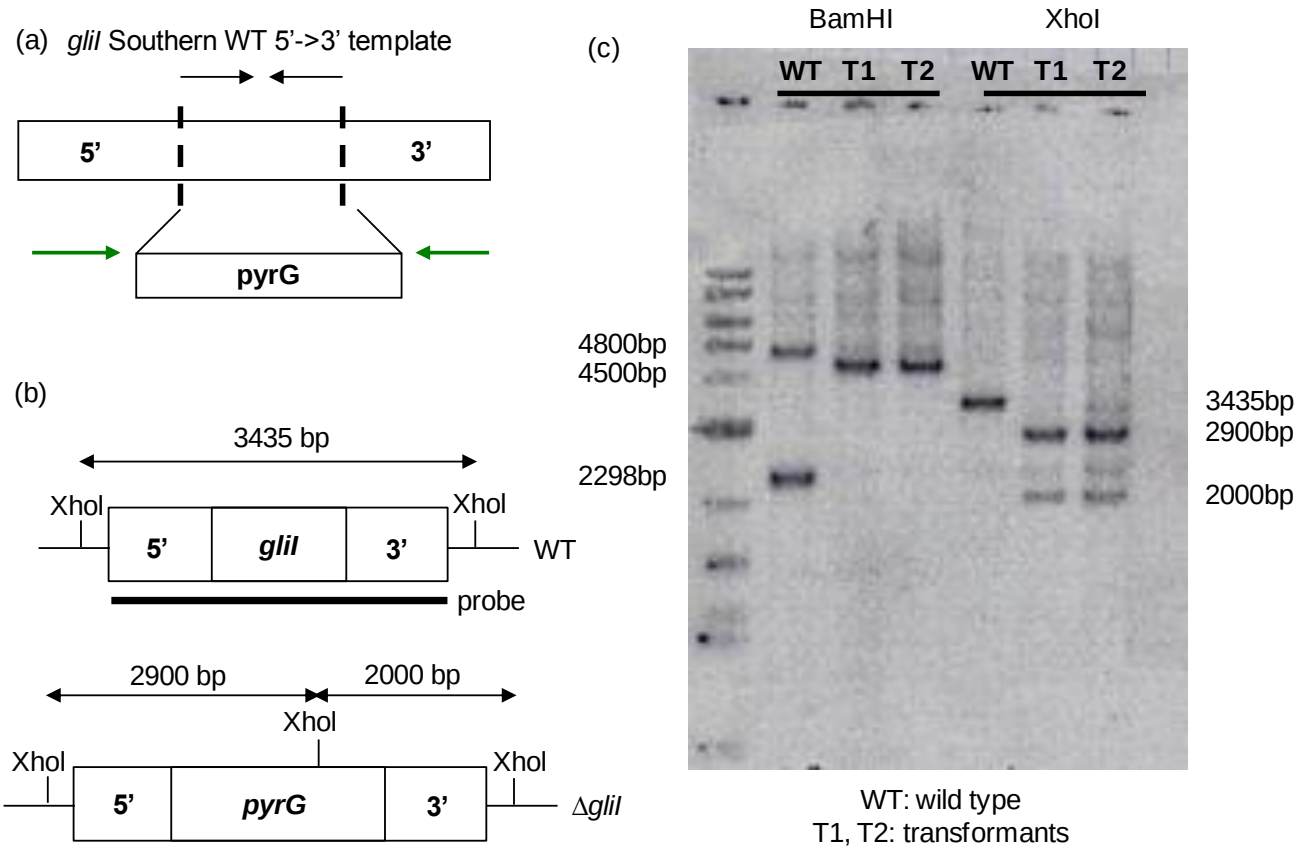

Figure S4. The construction of Δ*gliI* mutants was confirmed by Southern analysis of genomic DNA from WT and two transformants (T1 and T2), indicating *gliI* replacement by *pyrG* in T1 and T2. (a) Wild type and two *gliI* replacement strains were probed with a 3435 bp fragment of DNA covering approximately 1 kb up and down stream of *gliI* ORF as well as the *gliI* ORF. (b) XhoI does not cut within the *gliI* ORF, rather XhoI cuts regions flanking *gliI* generating a single DNA fragment of 3435 bp. The DNA from transformants in which *pyrG* replaces *gliI* is cut by XhoI into two fragment of 2900 and 2000 bp each. (c) Southern blot analysis of WT and T1 and T2 after DNA treatment with BamHI and XhoI agree with predicted XhoI treatment DNA restriction products, confirming that *gliI* is present in WT and has been replaced by *pyrG* in T1 and T2.

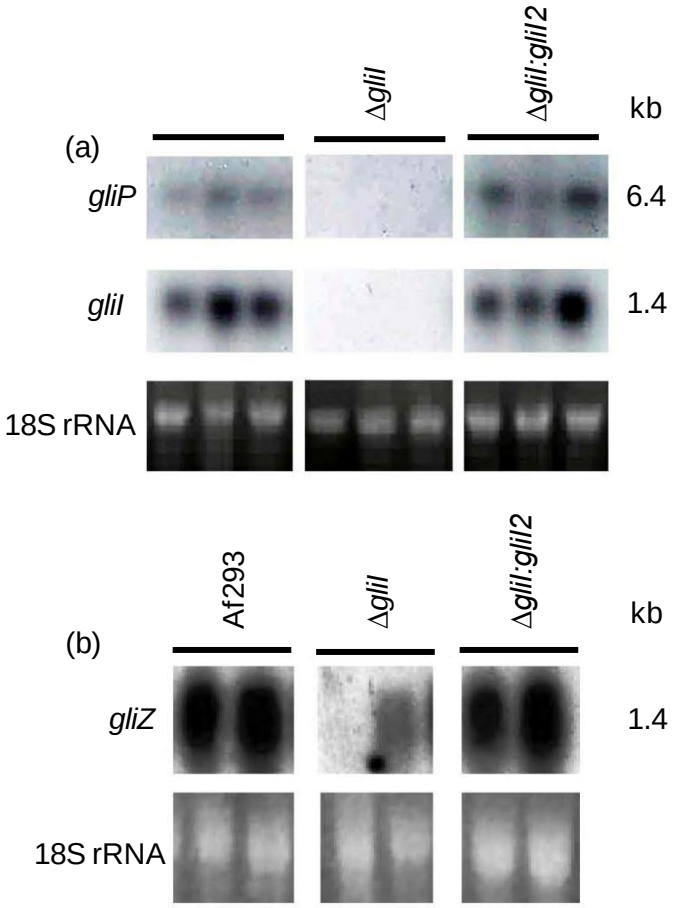

Figure S5. Total RNA was extracted from shaking cultures grown in Czapek Dox medium at 37 °C for two days. RNA was probed with a fragment of gliotoxin biosynthetic genes *gliP* (173 bp), *gliI* (653 bp) (a) and *gliZ* (1211 bp) (b)**.** Transcript sizes are marked. Ethidium bromide-stained 18S rRNA is shown as a control for RNA loading. (a) Transcripts of *gliP* and *gliI* were undetected in the *Δglil* mutant, but present in similar amounts in isolates Af293 and *Δglil:gliI*2. (b) Transcripts of *gliZ* were not detected in the *Δglil* mutant in one biological replicate and reduced in the second biological replicate, compared to that in Af293. The level of *gliZ* transcription was restored to wild type level in isolate *ΔgliI:gliI2* in both biological replicates.

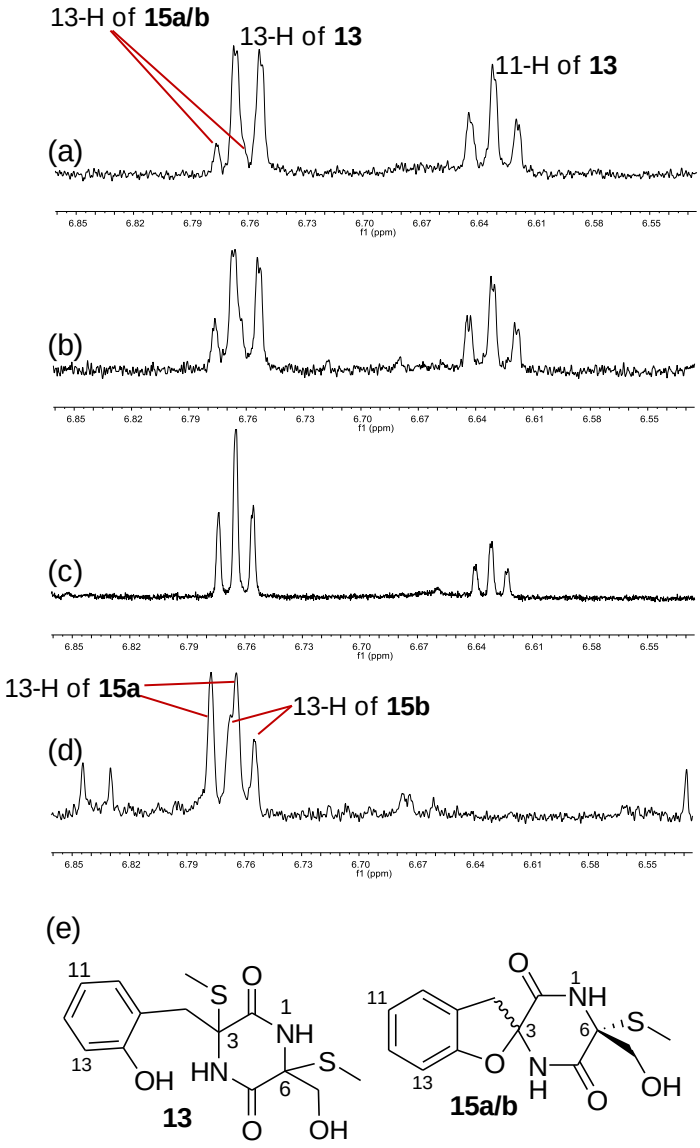

Figure S6. Formation of a mixture of diastereomers of spirocyclic **15** from diketopiperazine **13**. (a) 6.5-6.9 ppm section of the ^{1}H NMR spectrum of a sample of diketopiperazine **13**, showing signals for protons 11-H and 13-H of **13** in addition to a small signal for 13-H of **15a** and **15b** (600 MHz, DMSO-d_6). (b) Same sample after several days at room temp., showing increasing amounts of **15a/b** (600 MHz, DMSO-d_6). (c) After two weeks at room temp., most of **13** has converted to **15a/b** (900 MHz, DMSO-d_6). (d) Sample of a mixture of **15a** and **15b** (600 MHz, DMSO-d_6), containing small amounts of impurities (signals at 6.84 and 6.53 ppm). (e) Compounds **13** and **15a/b**.

Figure S7. GliP domain architecture including two adenylation (A), three thiolation (T), and two condensation domains.[4]

Table S1. ^{1}H (600 MHz) and ^{13}C (151 MHz) NMR spectroscopic data for compound **4** in DMSO-d_6. Chemical shifts were referenced to δ(C<u>H</u>D$_2$SOCD$_3$) = 2.50 ppm and δ(^{13}<u>C</u>HD$_2$SOCD$_3$) = 39.5 ppm. ^{13}C chemical shifts were determined via HMQC and HMBC spectra. (^{1}H,^{1}H)-coupling constants were determined from the ^{1}H-NMR spectrum or the dqfCOSY spectrum. HMBC correlations (optimized for 6 Hz) are from the proton(s) stated to the indicated carbon. ROESY correlations were observed using a mixing time of 275 ms. Abbreviation: wk = weak, but clearly discernable ROESY correlation.

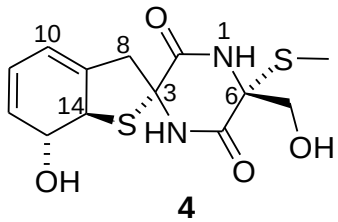

4

Position	**δ_C**	**Proton**	**δ_H (J_{HH} [Hz])**	**HMBC**	**ROESY**
1-NH		1-NH	9.32	3, 5	7-H$_a$, 6-S-CH$_3$
2	167.9				
3	69.6				
4-NH		4-NH	9.07	2, 5, 6, 8	8-H$_a$, 13-H (wk)
5	165.1				
6	65.3				
6-S-CH$_3$	12.2	6-S-CH$_3$	2.12		7-H$_a$ 7-H$_b$, 14-H (wk)
7	63.6	7-H$_a$	3.57 ($J_{7\text{-Ha},7\text{-Hb}}$ = 11)	5, 6	7-H$_b$
		7-H$_b$	3.88	2, 5, 6	
8	44.7	8-H$_a$	2.89 ($J_{8\text{-Ha},8\text{-Hb}}$ = 16, $J_{8\text{-Ha},10\text{-H}}$ = 2, $J_{8\text{-Ha},12\text{-H}}$ <1, $J_{8\text{-Ha},13\text{-H}}$ < 1)	2, 3, 9, 10, 14	7-H$_b$, 10-H
		8-H$_b$	3.40 ($J_{8\text{-Hb},10\text{-H}}$ = 2, $J_{8\text{-Ha},12\text{-H}}$ <1, $J_{8\text{-Hb},13\text{-H}}$ < 1, $J_{8\text{-Hb},14\text{-H}}$ = 2)	2, 3, 9, 10, 15	14-H, 10-H
9	141.1				
10	115.8	10-H	5.77 ($J_{10\text{-H},11\text{-H}}$ = 6.7)	14	11-H
11	123.9	11-H	5.85 ($J_{11\text{-H},12\text{-H}}$ = 10, $J_{11\text{-H},13\text{-H}}$ = 3)	9	12-H
12	133.1	12-H	5.66 ($J_{12\text{-H},13\text{-H}}$ = 3, $J_{12\text{-H},14\text{-H}}$ < 1)	10, 13, 14	13-H
13	73.3	13-H	4.44 ($J_{13\text{-H},14\text{-H}}$ = 15)	9, 14	
14	57.1	14-H	4.21	9, 13	7-H$_a$, 6-S-CH$_3$

Table S2. ^{1}H (600 MHz) and ^{13}C (151 MHz) NMR spectroscopic data for compound **5** in acetonitrile-d_3. Chemical shifts were referenced to δ(C<u>H</u>D$_2$CN) = 1.94 ppm and δ(^{13}<u>C</u>HD$_2$CN) = 1.3 ppm. ^{13}C chemical shifts were determined via HMQC and HMBC spectra. (^{1}H,^{1}H)-coupling constants were determined from the ^{1}H-NMR spectrum or the dqfCOSY spectrum. HMBC correlations (optimized for 6 Hz) are from the proton(s) stated to the indicated carbon. Abbreviation: wk = weak, but clearly discernable HMBC.

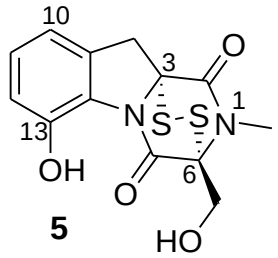

5

Position	**δ_C**	**Proton**	**δ_H (J_{HH} [Hz])**	**HMBC**
1-N				
1-N-CH_3	27.8	1-N-CH_3	3.20	2, 6
2	165.9			
3	74.6			
4-N				
5	162.7			
6	78.1			
7	60.4	7-H_a	4.35 ($J_{7\text{-Ha},7\text{-Hb}}$ = 13)	5, 6
		7-H_b	4.46	5
7-OH		7-OH		
8	36.9	8-H_a	3.40 ($J_{8\text{-Ha},8\text{Hb}}$ = 19, $J_{8\text{-Ha},10\text{-H}}$ < 1, $J_{8\text{-Ha},12\text{-H}}$ < 1)	2, 3, 8, 9, 10, 11(wk), 14
		8-H_b	4.19 ($J_{8\text{-Hb},10\text{-H}}$ < 1, $J_{8\text{-Hb},12\text{-H}}$ < 1)	2, 3, 8, 9, 10, 11(wk), 13, 14
9	132.0			
10	117.1	10-H	6.88 ($J_{10\text{-H},11\text{-H}}$ = 8)	8, 14
11	129.6	11-H	7.16 ($J_{11\text{-H},12\text{-H}}$ = 7)	9, 13
12	117.9	12-H	6.83	14
13	145.9			
13-OH		13-OH	10.73	11(wk), 12, 13, 14
14	124.9			

Table S3. ^{1}H (600 MHz) and ^{13}C (151 MHz) NMR spectroscopic data for compound **9** in acetonitrile-d_3. Chemical shifts were referenced to δ(C<u>H</u>D$_2$CN) = 1.94 ppm and δ(^{13}<u>C</u>HD$_2$CN) = 1.3 ppm. ^{13}C chemical shifts were determined via HMQC and HMBC spectra. (^{1}H,^{1}H)-coupling constants were determined from the ^{1}H-NMR spectrum or the dqfCOSY spectrum. HMBC correlations (optimized for 6 Hz) are from the proton(s) stated to the indicated carbon. Abbreviation: wk = weak, but clearly discernable HMBC.

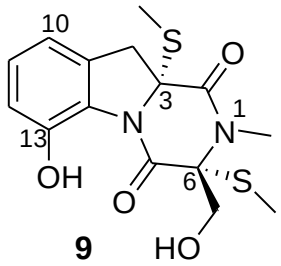

9

Position	**δ_C**	**Proton**	**δ_H (J_{HH} [Hz])**	**HMBC**
1-N				
1-N-CH_3	29.0	1-N-CH_3	3.12	2, 6
2	165.8			
3	72.1			
3-S-CH_3	14.8	3-S-CH_3	2.21	3
4-N				
5	165.7			
6	73.4			
6-S-CH_3	13.6	6-S-CH_3	2.31	6
7	64.4	7-H_a	3.91 ($J_{7\text{-Ha},7\text{-Hb}}$ = 12, $J_{7\text{-Ha},7\text{-OH}}$ = 2)	2, 6
		7-H_b	4.29 ($J_{7\text{-Hb},7\text{-OH}}$ = 2)	2
7-OH		7-OH	5.74	
8	40.0	8-H_a	3.47 ($J_{8\text{-Ha},8\text{Hb}}$ = 17, $J_{8\text{-Ha},10\text{-H}}$ < 1, $J_{8\text{-Ha},12\text{-H}}$ < 1)	3, 9, 10, 14
		8-H_b	3.55 ($J_{8\text{-Hb},10\text{-H}}$ < 1, $J_{8\text{-Hb},12\text{-H}}$ = < 1)	2, 3, 9, 10, 13(wk), 14
9	132.9			
10	117.4	10-H	6.90 ($J_{10\text{-H},11\text{-H}}$ = 8)	8, 12, 13, 14
11	129.8	11-H	7.19 ($J_{11\text{-H},12\text{-H}}$ = 7)	9, 13
12	118.1	12-H	6.86	10, 13, 14
13	147.3			
13-OH		13-OH	10.27	11, 12, 13, 14
14	128.6			

Table S4a. ^{1}H (600 MHz) and ^{13}C (151 MHz) NMR spectroscopic data for compound **12** in acetonitrile-d_3. Chemical shifts were referenced to δ(C<u>H</u>D$_2$CN) = 1.94 ppm and δ(^{13}<u>C</u>HD$_2$CN) = 1.3 ppm. ^{13}C chemical shifts were determined via HSQCAD and HMBC spectra. (^{1}H,^{1}H)-coupling constants were determined from the ^{1}H-NMR spectrum or the dqfCOSY spectrum. HMBC correlations (optimized for 6 Hz) are from the proton(s) stated to the indicated carbon.

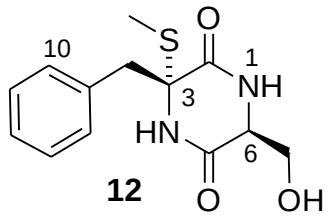

12

Position	**δ_C**	**Proton**	**δ_H (J_{HH} [Hz])**	**HMBC**
1-NH		1-NH	6.40 or 6.85	
2	166.2			
3	69.1			
3-S-CH_3	13.2		2.18	3
4-NH		4-NH	6.40 or 6.85	
5	166.5			
6	57.6	6-H	3.15 ($J_{6\text{-H,7-Ha}}$ = 7, $J_{6\text{-H,7-Hb}}$ = 6)	5
7	63.5	7-H_a	3.53 ($J_{7\text{-Ha,7-Hb}}$ = 12, $J_{7\text{-Ha,7-OH}}$ = 8)	
		7-H_b	3.66	
7-OH		7-OH	3.17	
8	45.6	8-H_a	2.96 ($J_{8\text{-Ha,8-Hb}}$ = 13)	2, 3, 9, 10, 14
		8-H_b	3.51	3, 9, 10, 14
9	135.7			
10, 14	131.5	10-H, 14-H	7.25	8, 10, 12, 14
11, 13	129.1	11-H, 13-H	7.30	9, 11, 13
12	128.6	12-H	7.27	10, 14

Table S4b. ^{1}H (600 MHz) NMR spectroscopic data for compound **12** in DMSO-d_6. Chemical shifts were referenced to δ(C<u>H</u>D$_2$SOCD$_3$) = 2.50 ppm. (^{1}H,^{1}H)-coupling constants were determined from the ^{1}H-NMR spectrum. ROESY correlations were observed using a mixing time of 350 ms. Coupling multiplicities are annotated as: s, singlet; d, doublet; dd, doublet of doublets; m, multiplet.

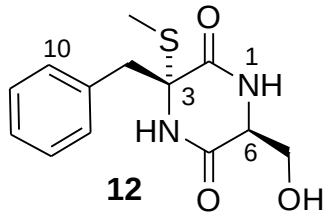

12

Position	**Proton**	**δ_H (J [Hz])**	**ROESY**
1-NH	1-NH	8.04 (s)	6-H, 7-H$_a$, 7-OH
2			
3			
3-S-CH$_3$	3-S-CH$_3$	2.18 (s)	4-H, 8-H$_b$, 7-OH
4-NH	4-NH	8.80 (s)	8-H$_a$, aromatic-H (7.20)
5			
6	6-H	3.14 (m)	7-OH
7	7-Ha	3.42 (m)	7-H$_b$, 7-OH
	7-Hb	3.63 (m)	7-H$_a$, 7-OH
7-OH	7-OH	4.96 (dd, J = 5, J = 6) (No signal upon D$_2$O addition)	
8	8-Ha	2.92 (d, J = 13)	8-H$_b$, aromatic-H (7.24)
	8-Hb	3.41 (d, J = 13)	8-H$_a$, aromatic-H (7.24)
9			
phenyl		7.25 - 7.21	

Table S5. ^{1}H (900 MHz) and ^{13}C (227 MHz) NMR spectroscopic data for compound **13** in DMSO-d_6. Chemical shifts were referenced to δ(C<u>H</u>D$_2$SOCD$_3$) = 2.50 ppm and δ(^{13}<u>C</u>HD$_2$SOCD$_3$) = 39.5 ppm. ^{13}C chemical shifts were determined via gHMQC and gHMBCAD spectra. (^{1}H,^{1}H)-coupling constants were determined from the ^{1}H-NMR spectrum. Coupling multiplicities are annotated as: s, singlet; d, doublet; dd, doublet of doublets; and t, triplet. ROESY correlations were observed using a mixing time of 250 ms. gHMBCAD correlations (optimized for 6 Hz) are from the proton(s) stated to the indicated carbon.

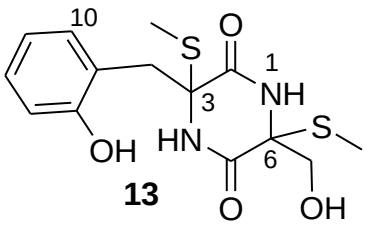

13

Position	**δ$_C$**	**Proton**	**δ$_H$ (*J* [Hz])**	**ROESY**	**gHMBC**
1-NH		1-NH	8.67 (s)	6-S-CH$_3$	3, 5
2	165.7				
3	65.0				
3-S-CH$_3$	13.0	3-S-CH$_3$	2.25 (s)		3
4-NH		4-NH	8.51 (s)	3-S-CH$_3$, 10-H	2, 6
5	165.3				
6	65.6				
6-S-CH$_3$	14.4	6-S-CH$_3$	2.14 (s)		6
7	64.6	7-H$_a$	3.45 (dd, $J_{7Ha,7Hb}$ = 11, $J_{7Ha,OH}$ = 6)	7-OH	5, 6
		7-H$_b$	3.65 (dd, $J_{7Ha,7Hb}$ = 11, $J_{7Hb,OH}$ = 6)	7-OH	
7-OH		7-OH	5.14 (t, J = 6)		
8	45.9	8-H$_a$	3.16 (d, $J_{8Ha,8Hb}$ = 15)		2, 3, 9, 14
		8-H$_b$	3.41 (d, $J_{8Ha,8Hb}$ = 15)	10-OH	10
9	122.0				
10	130.3	10-H	7.20 (d, J = 8)	8-H$_a$, 8-H$_b$	12
11	118.6	11-H	6.63 (t, J = 8)	10-H	9, 13
12	127.5	12-H	7.00 (t, J = 8)	11-H	10
13	114.9	14-H	6.76 (d, J = 8)	12-H, 10-OH,	11
14	155.3				
14-OH		14-OH	9.41 (s)	13-H	9, 14

Table S6a. ^{1}H (600 MHz) and ^{13}C (151 MHz) NMR spectroscopic data for compound **14a** in acetonitrile-d_3. Chemical shifts were referenced to δ(C<u>H</u>D$_2$CN) = 1.94 ppm and δ(^{13}<u>C</u>HD$_2$CN) = 1.3 ppm. (^{1}H,^{1}H)-coupling constants were determined from the ^{1}H-NMR spectrum or the dqfCOSY spectrum. ^{13}C chemical shifts were determined via HSQCAD and HMBC spectra. HMBC correlations (optimized for 6 Hz) are from the proton(s) stated to the indicated carbon.

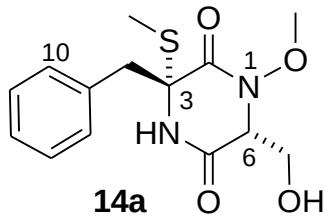

14a

Position	**δ_C**	**Proton**	**δ_H (J_{HH} [Hz])**	**HMBC**
1-N				
1-N-O-CH_3	62.0	1-N-O-CH_3	3.52	
2	163.0			
3	68.8			
3-S-CH_3	13.4	3-S-CH_3	2.19	3
4-NH		4-NH	7.02	
5	165.2			
6	63.3	6-H	3.46 ($J_{6\text{-H},7\text{-Ha}}$ = 5, $J_{6\text{-H},7\text{-Hb}}$ = 5)	5
7	59.2	7-H_a	3.77 ($J_{7\text{-Ha},7\text{-OH}}$ = 6)	5
		7-H_b	3.78 ($J_{7\text{-Hb},7\text{-OH}}$ = 6)	
7-OH		7-OH	3.12	
8	46.9	8-H_a	3.00 ($J_{8\text{-Ha},8\text{-Hb}}$ = 13)	2, 3, 9, 10, 14
		8-H_b	3.51	2, 3, 9, 10, 14
9	135.3			
10, 14	131.7	10-H, 14-H	7.20	8, 12, 11, 10, 13, 14
11, 13	129.4	11-H, 13-H	7.30	9, 11, 13
12	128.5	12-H	7.28	

Table S6b. ^{1}H (600 MHz), and ^{15}N (62 MHz) spectroscopic data for compound **14a** DMSO-d_6. Chemical shifts were referenced to δ($C\underline{H}D_2SOCD_3$) = 2.50 ppm. (^{1}H,^{1}H)-Coupling constants were determined from the ^{1}H-NMR spectrum. Coupling multiplicity are annotated as: s, singlet; d, doublet; ddd, doublet of doublets of doublets; t, triplet; m, multiplet. ROESY correlations were observed using a mixing time of 250 ms. ^{15}N-gHMBCAD correlations (optimized for 8 Hz) are from the proton(s) stated to the indicated nitrogen.

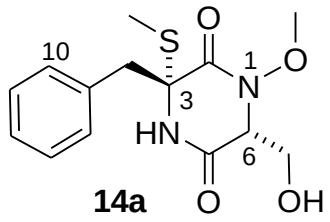

14a

Position	**Proton**	**δ_H (*J* [Hz])**	**ROESY**	**^{15}N-gHMBC**	**δ ^{15}N**
1-N					185.4
1-N-O-CH_3		3.44 (s)	aromatic-H (7.18 ppm)	1-N	
2					
3					
3-S-CH_3		2.17 (s)	4-H, 8-H_a, 8-H_b, 7-OH		
4-NH	4-NH	9.00 (s)	8-H_a, aromatic-H (7.18 ppm)	4-NH (residual 1 bond)	130.0
5					
6		3.57 (t, *J* = 2)	7-H_a, 7-H_b, 7-OH		
7	7-H_a	3.62 (ddd, *J* = 11, *J* = 5, *J* = 3)	7-H_b		
	7-H_b	3.67 (ddd, *J* = 11, *J* = 5, *J* = 2)	7-H_a		
7-OH	7-OH	5.11 (t, *J* = 5)			
8	8-H_a	2.99 (d, *J* = 13)	8-H_b, aromatic-H (7.18 ppm, 7.22 ppm)		
	8-H_b	3.38 (d, *J* = 13)	8-H_a, aromatic-H (7.18 ppm, 7.22 ppm)	4-N	
9					
phenyl		7.28-7.19 (m)			

Table S7a. ^{1}H (600 MHz) and ^{13}C (151 MHz) NMR spectroscopic data for compound **14b** in acetonitrile-d_3. Chemical shifts were referenced to δ(C<u>H</u>D_2CN) = 1.94 ppm and δ(^{13}<u>C</u>HD_2CN) = 1.3 ppm. ^{13}C chemical shifts were determined via HSQCAD and HMBC spectra. (^{1}H,^{1}H)-coupling constants were determined from the ^{1}H-NMR spectrum or the dqfCOSY spectrum. HMBC correlations (optimized for 6 Hz) are from the proton(s) stated to the indicated carbon.

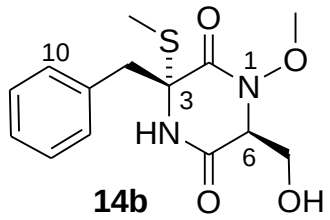

14b

Position	**δ_C**	**Proton**	**δ_H (J_{HH} [Hz])**	**HMBC**
1-N				
1-N-O-CH_3	62.9	1-N-O-CH_3	3.74	
2	163.8			
3	68.2			
3-S-CH_3	13.1	3-S-CH_3	2.14	3
4-NH		4-NH	6.75	
5	165.9			
6	64.6	6-H	4.28 ($J_{6\text{-H},7\text{-Ha}}$ = 4, $J_{6\text{-H},7\text{-Hb}}$ = 3)	5
7	60.1	7-H_a	3.56 ($J_{7\text{-Ha},7\text{-Hb}}$ = 12, $J_{7\text{-Ha},\ 7\text{-OH}}$ = 6)	
		7-H_b	3.61 ($J_{7\text{-Hb},7\text{-OH}}$ = 6)	
7-OH		7-OH	2.78	
8	44.9	8-H_a	3.11 ($J_{8\text{-Ha},8\text{-Hb}}$ = 14)	2, 3, 9, 10
		8-H_b	3.55	
9	135.3			
10,14	132.0	10-H, 14-H	7.24	8, 10, 14, 12
11,13	129.2	11-H, 13-H	7.30	
12	128.3		7.26	

Table S7b. ^{1}H (600 MHz), and ^{15}N (62 MHz) spectroscopic data for compound **14b** DMSO-d_6. Chemical shifts were referenced to δ($C\underline{H}D_2SOCD_3$) = 2.50 ppm . (^{1}H,^{1}H)-Coupling constants were determined from the ^{1}H-NMR spectrum. Coupling multiplicity are annotated as: s, singlet; d, doublet; t, triplet; and m, multiplet. ROESY correlations were observed using a mixing time of 250 ms. ^{15}N-gHMBCAD correlations (optimized for 8 Hz) are from the proton(s) stated to the indicated nitrogen.

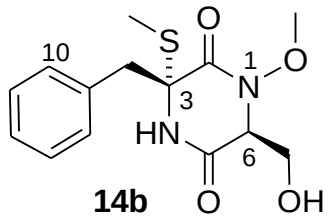

14b

Position	**Proton**	**δ_H (*J* [Hz])**	**ROESY**	**^{15}N-gHMBC**	**δ ^{15}N**
1-N					184.5
1-N-O-CH_3	1-N-O-CH_3	3.67 (s)	6-H, 3-S-CH3,	1-N	
2					
3					
3-S-CH_3	3-S-CH_3	2.15 (s)	6-H		
4-NH		8.85 (s)	8-H_a, 8-H_b, aromatic-H (7.20 ppm)		
5					
6	6-H	4.32 (broad-t, *J* = 3)	7-H_a, 7-H_b		
7	7-H_a	3.51 (m)	7-H_b, 7-OH		
	7-H_b	3.51 (m)	7-H_a, 7-OH		
7-OH	7-OH	4.67 (t, *J* = 5) (No signal upon D2O addition)			
8	8-H_a	3.03 (d, *J* = 14)	aromatic-H (7.20 ppm)		
	8-H_b	3.49 (d, *J* = 14)	aromatic-H (7.20 ppm)		
9					
phenyl		7.23-7.19 (m)			

Table S8. ^{1}H (600 MHz) and ^{13}C (151 MHz) NMR spectroscopic data for compound **15a** (major diastereomer, diastereomeric ratio **15a**:**15b** = 6:4) in DMSO-d_6. Chemical shifts were referenced to δ(C<u>H</u>D_2SOCD_3) = 2.50 ppm and δ(^{13}<u>C</u>HD_2SOCD_3) = 39.5 ppm. ^{13}C chemical shifts were determined via HMQC and HMBC spectra. (^{1}H,^{1}H)-coupling constants were determined from the ^{1}H-NMR spectrum or the dqfCOSY spectrum. HMBC correlations (optimized for 6 Hz) are from the proton(s) stated to the indicated carbon.

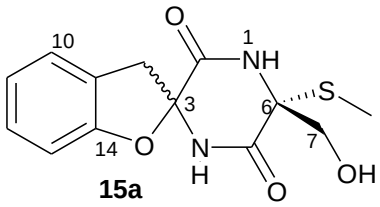

15a

Position	**δ_C**	**Proton**	**δ_H (J_{HH} [Hz])**	**HMBC**
1-NH		1-NH	9.06	3, 5
2	164.7			
3	91.8			
4-NH		4-NH	9.61	2, 6
5	165.8			
6	66.2			
6-S-CH_3	12.2	6-S-CH_3	2.19	6
7	64.6	7-H_a	3.53 ($J_{7\text{-Ha},7\text{-Hb}}$ = 11, $J_{7\text{-Ha},7\text{-OH}}$ = 5)	5
		7-H_b	3.89 ($J_{7\text{-Hb},7\text{-OH}}$ = 6	
7-OH		7-OH	5.41	6
8	38.5	8-H_a	3.19 ($J_{8\text{-Ha},8\text{-Hb}}$ = 16)	2, 3, 9, 14
		8-H_b	3.83	2, 9, 14
9	125.4			
10	124.3	10-H	7.23 ($J_{10\text{-H},11\text{-H}}$ = 7)	12
11	120.9	11-H	6.89 ($J_{11\text{-H},12\text{-H}}$ = 7)	9, 13
12	127.7	12-H	7.13 ($J_{12\text{-H},13\text{-H}}$ = 7)	10, 14
13	108.7	13-H	6.77	9, 11
14	156.9	14-H		

Table S9. ^{1}H (600 MHz) and ^{13}C (151 MHz) NMR spectroscopic data for compound **15b** (minor diastereomer, diastereomeric ratio **15a**:**15b** = 6:4) in DMSO-d_6. Chemical shifts were referenced to δ(C<u>H</u>D_2SOCD_3) = 2.50 ppm and δ(^{13}<u>C</u>HD_2SOCD_3) = 39.5 ppm. ^{13}C chemical shifts were determined via HMQC and HMBC spectra. (^{1}H,^{1}H)-coupling constants were determined from the ^{1}H-NMR spectrum or the dqfCOSY spectrum. HMBC correlations (optimized for 6 Hz) are from the proton(s) stated to the indicated carbon

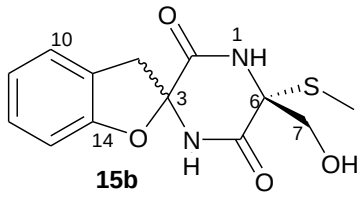

15b

Position	**δ_C**	**Proton**	**δ_H (J_{HH} [Hz])**	**HMBC**
1-NH		1-NH	8.99	3, 5
2	164.8			
3	91.5			
4-NH		4-NH	9.56	2, 6
5	165.1			
6	68.2			
6-S-CH_3	11.6	6-S-CH_3	2.07	6
7	64.6	7-H_a	3.52 ($J_{7\text{-Ha},7\text{-Hb}}$ = 11, $J_{7\text{-Ha},7\text{-OH}}$ = 5)	5
		7-H_b	3.89 ($J_{7\text{-Hb},7\text{-OH}}$ = 6	
7-OH		7-OH	5.54	
8	40.3	8-H_a	3.23 ($J_{8\text{-Ha},8\text{-Hb}}$ = 16)	2, 9, 14
		8-H_b	3.74	
9	125.5			
10	124.3	10-H	7.20 ($J_{10\text{-H},11\text{-H}}$ = 7)	12
11	120.8	11-H	6.88 ($J_{11\text{-H},12\text{-H}}$ = 7)	9, 13
12	127.9	12-H	7.13 ($J_{12\text{-H},13\text{-H}}$ = 7)	10, 14
13	108.5	13-H	6.76	9, 11
14	157.4	14-H		

Table S10. ^{1}H (900 MHz) and ^{13}C (227 MHz) NMR spectroscopic data for compound **16** in DMSO-d_6. Chemical shifts were referenced to δ(C<u>H</u>D_2SOCD_3) = 2.50 ppm and δ(^{13}<u>C</u>HD_2SOCD_3) = 39.5 ppm. ^{13}C chemical shifts were determined via gHMBCAD spectra. (^{1}H,^{1}H)-coupling constants were determined from the ^{1}H-NMR spectrum. Coupling multiplicities are annotated as: s, singlet; d, doublet; t, triplet; dt, doublet of triplets; and m, multiplet. gHMBCAD correlations (optimized for 6 Hz) are from the proton(s) stated to the indicated carbon. ROESY correlations were observed using a mixing time of 250 ms.

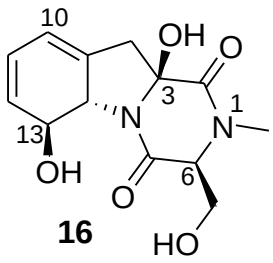

16

Position	**δ_C**	**Proton**	**δ_H (*J* [Hz])**	**gHMBC**	**ROESY**
1-N					
1-N-CH_3	32.0	1-N-CH_3	2.93	2, 6	6-H, 7-H
2	165.4				
3	88.9				
3-OH		3-OH	6.25 (d, *J* = 1)	8, 3	7-H_a, 7-H_b, 8-H_a
4-N					
5	168.6				
6	64.9	6-OH	4.21 (t, *J* = 3)	5	7-H_a, 7-H_b, 8-H_b
7	59.9	7-H_a	3.81 (dt, *J* = 4, *J* = 11)		7-OH
		7-H_b	3.91 (dt, *J* = 4, *J* = 11)		7-OH
7-OH		7-OH	6.47 (t, *J* = 4)	7, 6	
8	40.3	8-H_a	2.72 (d, *J* = 16)	3, 9, 10, 14	10-H, 14-H
		8-H_b	2.82 (d, *J* = 16)		10-H
9	117.8				
10	134.5	10-H	5.89 (m)		11-H
11	118.4	11-H	5.89 (m)		12-H
12	130.4	12-H	5.58 (m)	11	13-H
13	73.7	13-H	4.52 (d, *J* = 14)		13-OH
13-OH		13-OH	5.98 (s)	12, 13, 14	14-H
14	67.9	14-H	4.69 (d, *J* = 14)		

Table S11a. ^{1}H (600 MHz) and ^{13}C (151 MHz) NMR spectroscopic data for compound **17** in acetonitrile-d_3. Chemical shifts were referenced to δ(C<u>H</u>D$_2$CN) = 1.94 ppm and δ(^{13}<u>C</u>HD$_2$CN) = 1.3 ppm. ^{13}C chemical shifts were determined via HSQCAD and HMBC spectra. (^{1}H,^{1}H)-coupling constants were determined from the ^{1}H-NMR spectrum or the dqfCOSY spectrum. HMBC correlations (optimized for 6 Hz) are from the proton(s) stated to the indicated carbon.

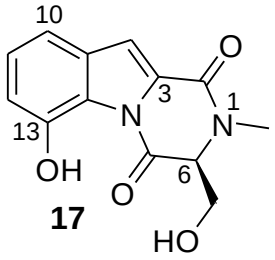

17

Position	**δ_C**	**Proton**	**δ_H (J_{HH} [Hz])**	**HMBC**
1-N				
1-N-CH_3	31.6	1-N-CH_3	3.07	2, 6
2	157.8			
3	117.7 (DMSO-d_6)			
4-N				
5	166.0			
6	67.0	6-H	4.32 ($J_{6\text{-H},7\text{-Ha}}$ = 2, $J_{6\text{-H},7\text{-Hb}}$ = 3)	2, 5
7	62.4	7-H_a	3.99 ($J_{7\text{-Ha},7\text{-Hb}}$ = 12, $J_{7\text{-Ha},7\text{-OH}}$ = 6)	
		7-H_b	4.08 ($J_{7\text{-Hb},7\text{-OH}}$ = 6)	
7-OH		7-OH	3.35	
8	110.1	8-H	7.36	9, 10, 13, 14
9	119.1			
10	108.9	10-H	7.90 ($J_{10\text{-H},11\text{-H}}$ = 8)	9, 12
11	129.8	11-H	7.34 ($J_{11\text{-H},12\text{-H}}$ = 9)	13, 14
12	110.6	12-H	6.81	9, 10, 14
13	151.9			
13-OH			7.70	
14	137.0			

Table S11b. ^{1}H (600 MHz) and ^{13}C (151 MHz) NMR spectroscopic data for compound **17** in DMSO-d_6. Chemical shifts were referenced to δ(C<u>H</u>D$_2$SOCD$_3$) = 2.50 ppm and δ(^{13}<u>C</u>HD$_2$SOCD$_3$) = 39.5 ppm. ^{13}C chemical shifts were determined via HMBC spectra and HSQCAD. HMBC correlations (optimized for 6 Hz) are from the proton(s) stated to the indicated carbon. (^{1}H,^{1}H)-coupling constants were determined from the ^{1}H-NMR spectrum. Coupling multiplicities are annotated as: s, singlet; d, doublet; t, triplet; dd, doublet of doublets; ddd, doublet of doublet of doublets; m, multiplet.

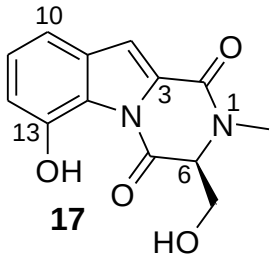

17

Position	**δ_C**	**Proton**	**δ_H (*J* [Hz])**	**HMBC**
1-N				
1-N-CH$_3$	30.5	1-N-CH$_3$	3.02 (s)	2, 6
2	156.3			
3	117.7			
4-N				
5	165.1			
6	65.8	6-H	4.49 (broad-t, *J* = 2)	5
7a	60.4	7-H$_a$	3.85 (ddd, *J* = 12, *J* = 6, *J* = 2)	
		7-H$_b$	3.98 (ddd, *J* = 11, *J* = 5, *J* = 3)	
7-OH		7-OH	5.36 (t, *J* = 6)	
8	108.7	8-H	7.33 (d, *J* < 1)	3, 11, 14
9	118.1			
10	106.6	10-H	7.79 (d, *J* = 8)	9, 12
11	128.5	11-H	7.31 (t, *J* = 8)	13, 14
12	109.7	12-H	6.76 (dd, *J* = 8, *J* < 1)	9, 10, 14
13	152.0			
13-OH			10, 19 (s)	9, 12, 13, 14
14	135.4			

Compound **4**, ^{1}H spectrurm, DMSO-d_6, 600MHz

4

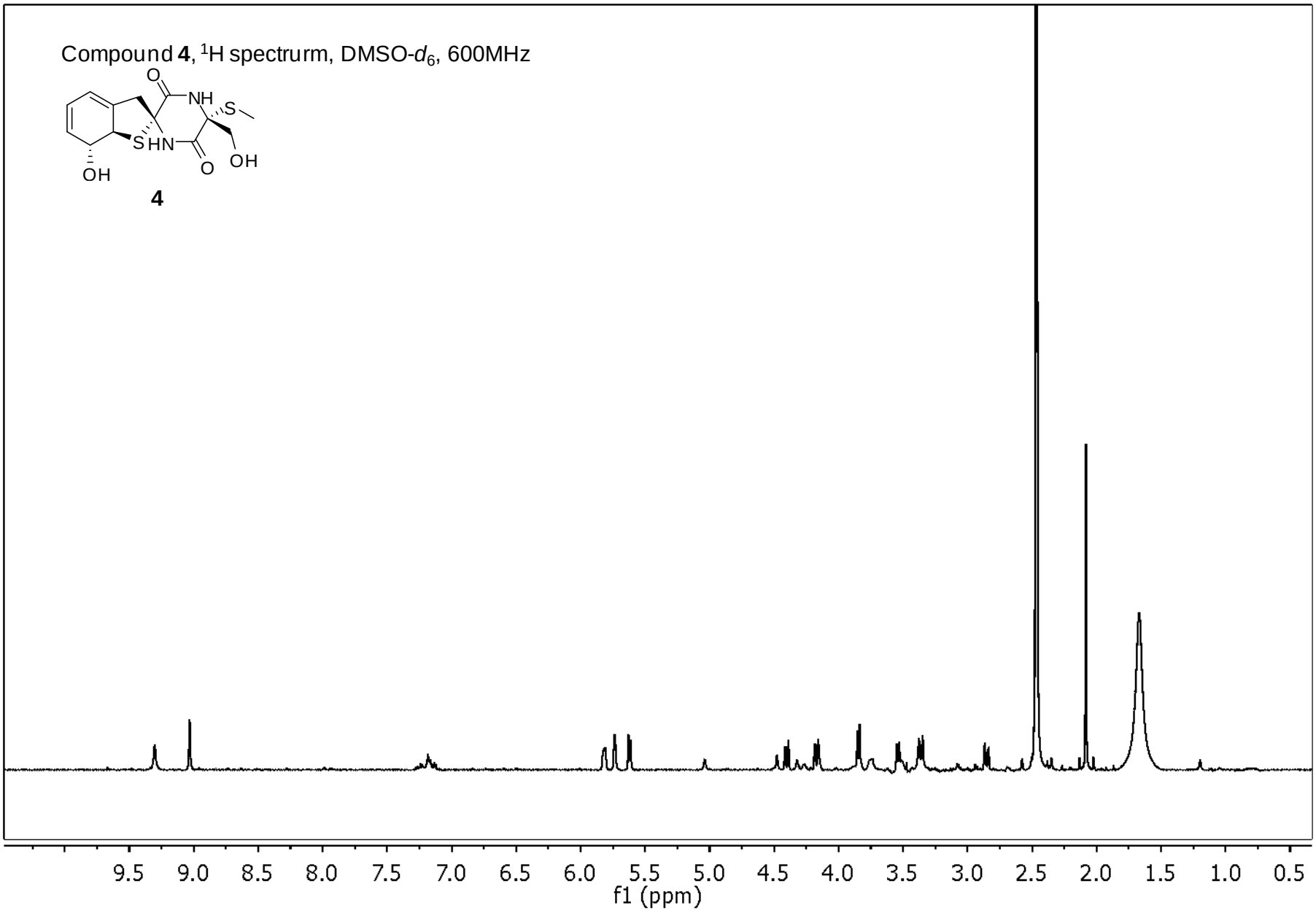

Compound **4**, dqfCOSY spectrum, DMSO-d_6, 600 MHz

4

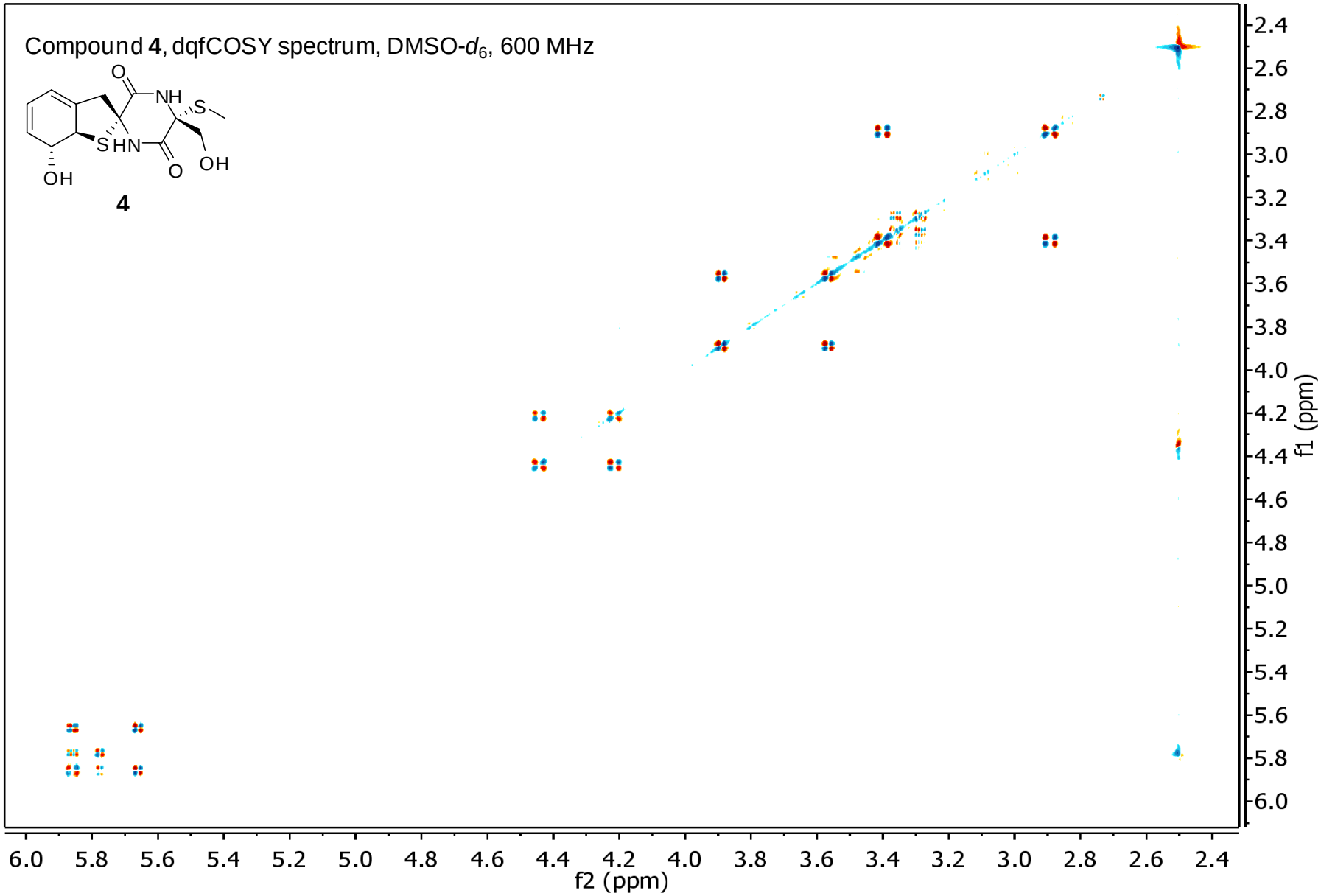

Compound **4**, dqfCOSY spectrum DMSO-d_6, 600 MHz, showing long-range couplings and impurities.

4

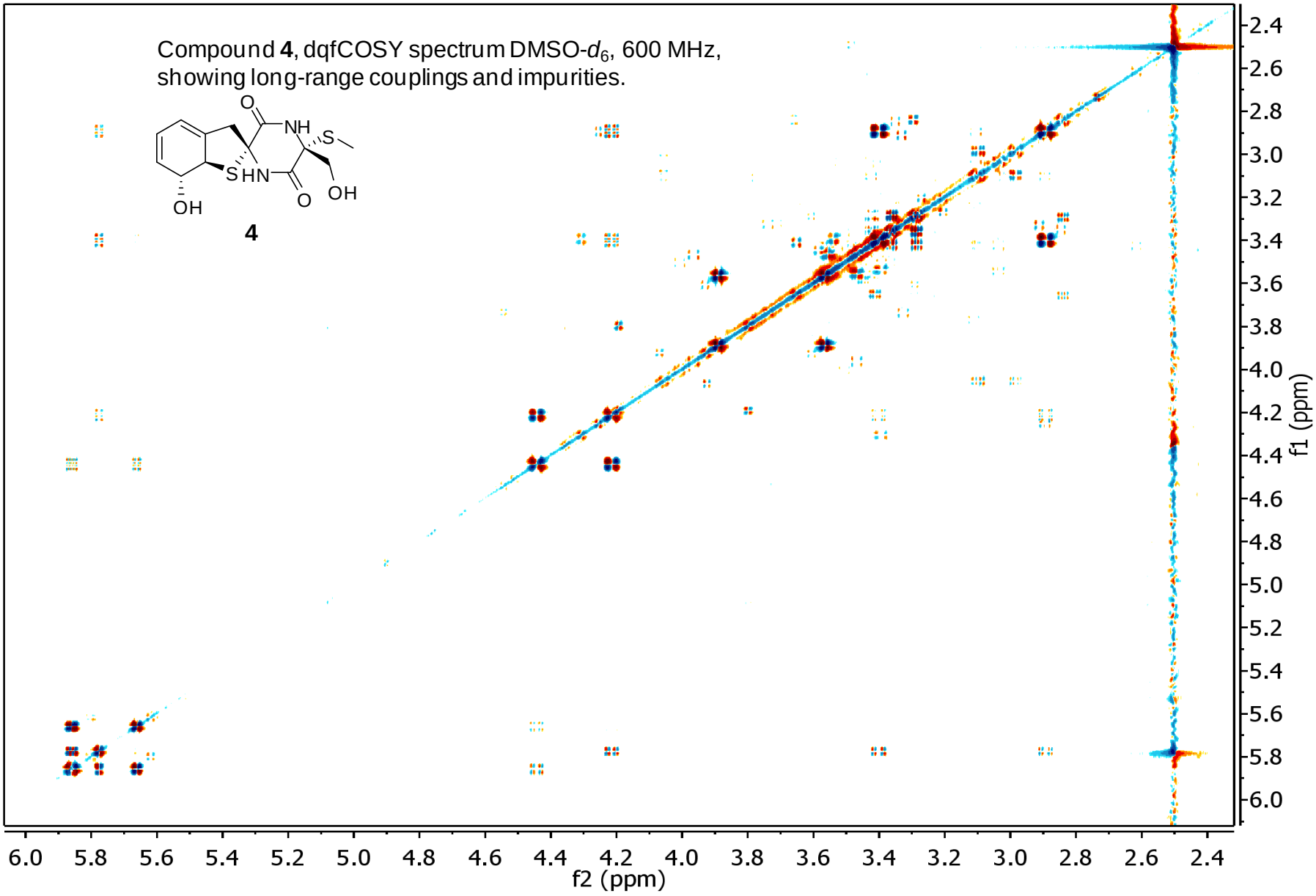

Compound **4**, HMQC spectrum, DMSO-d_6, 600 MHz

4

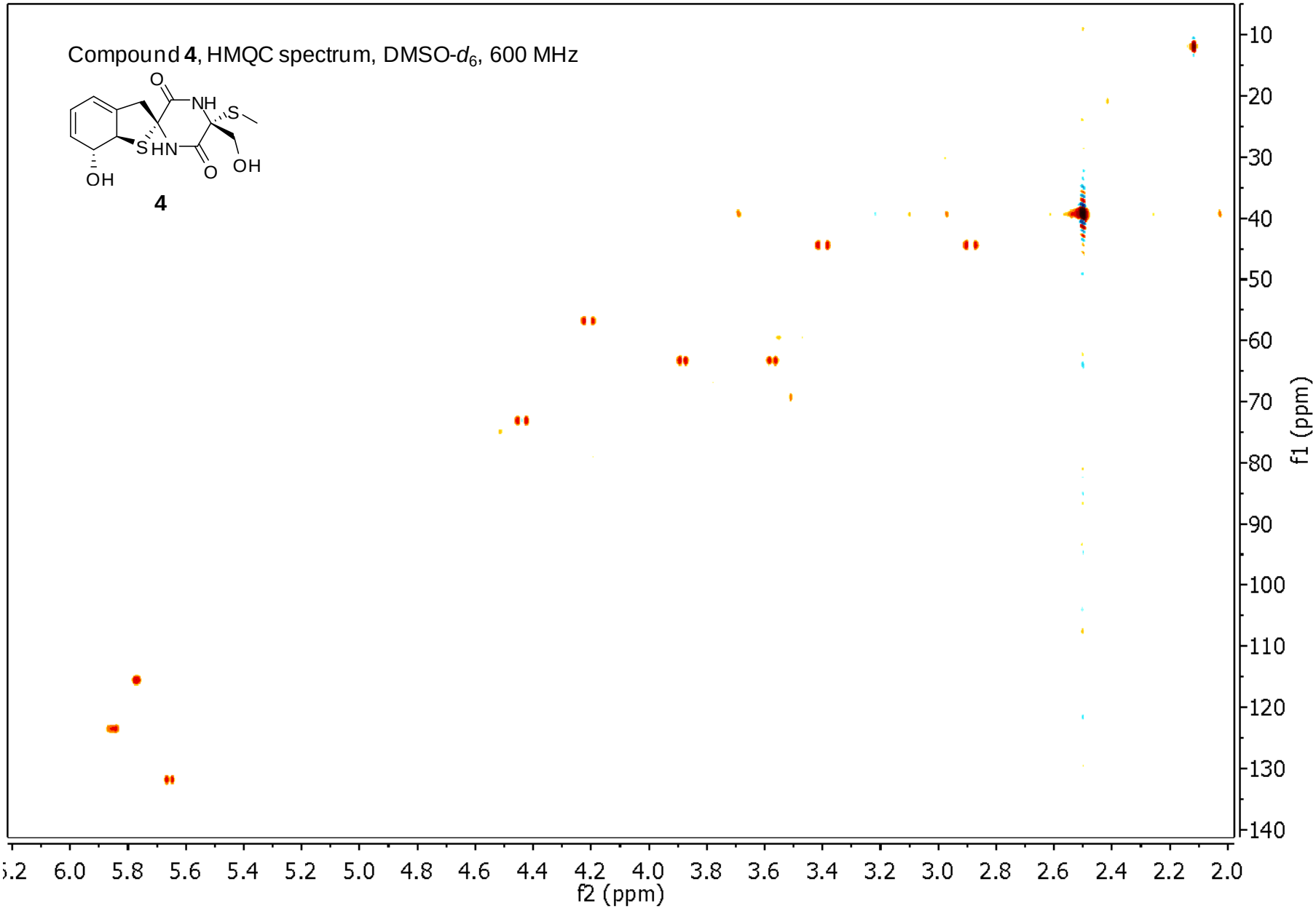

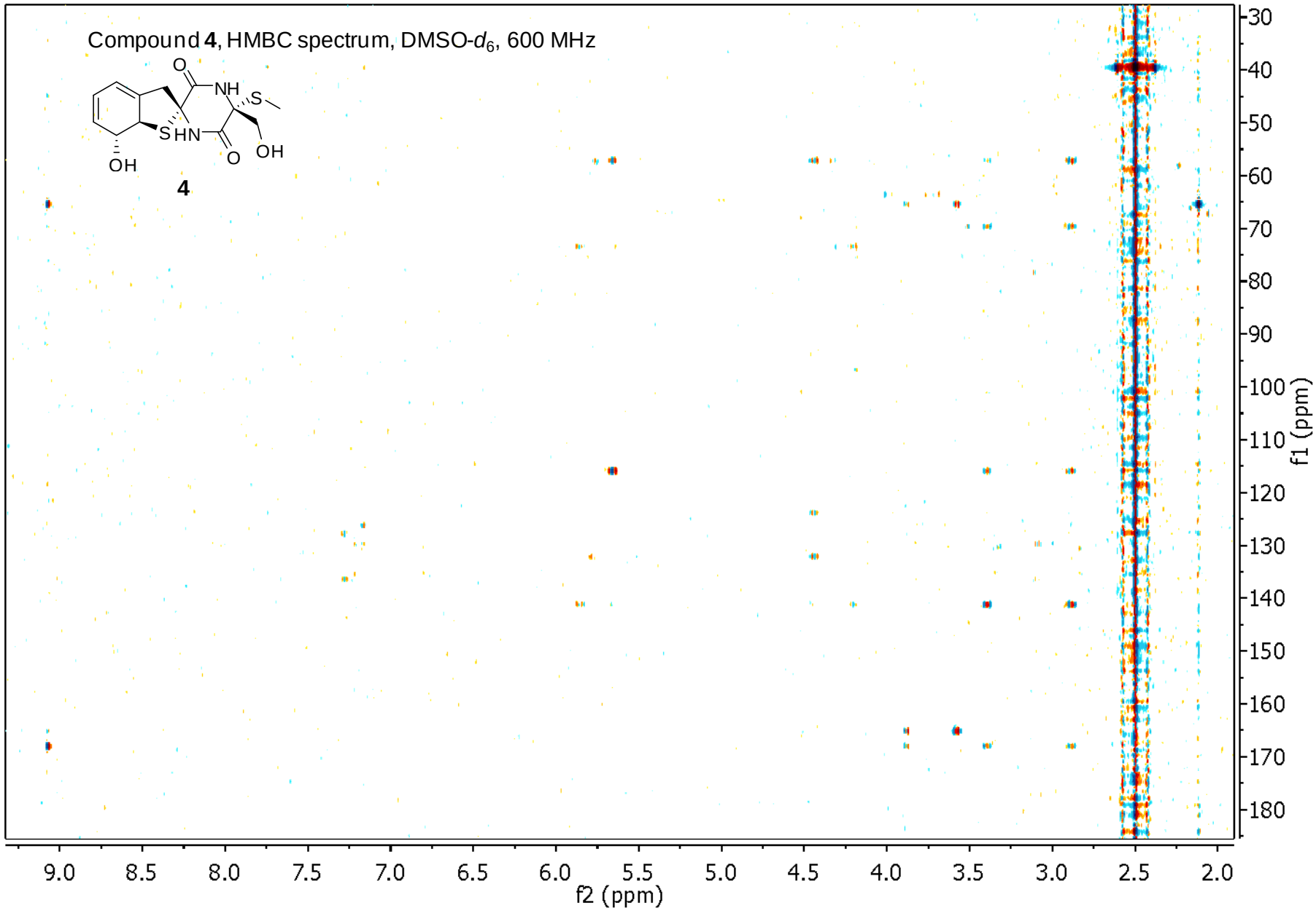
Compound 4, HMBC spectrum, DMSO-d6, 600 MHz
O
NH
S
S
HN
O
OH
OH
4
f2 (ppm)
f1 (ppm)
9.0
8.5
8.0
7.5
7.0
6.5
6.0
5.5
5.0
4.5
4.0
3.5
3.0
2.5
2.0
30
40
50
60
70
80
90
100
110
120
130
140
150
160
170
180

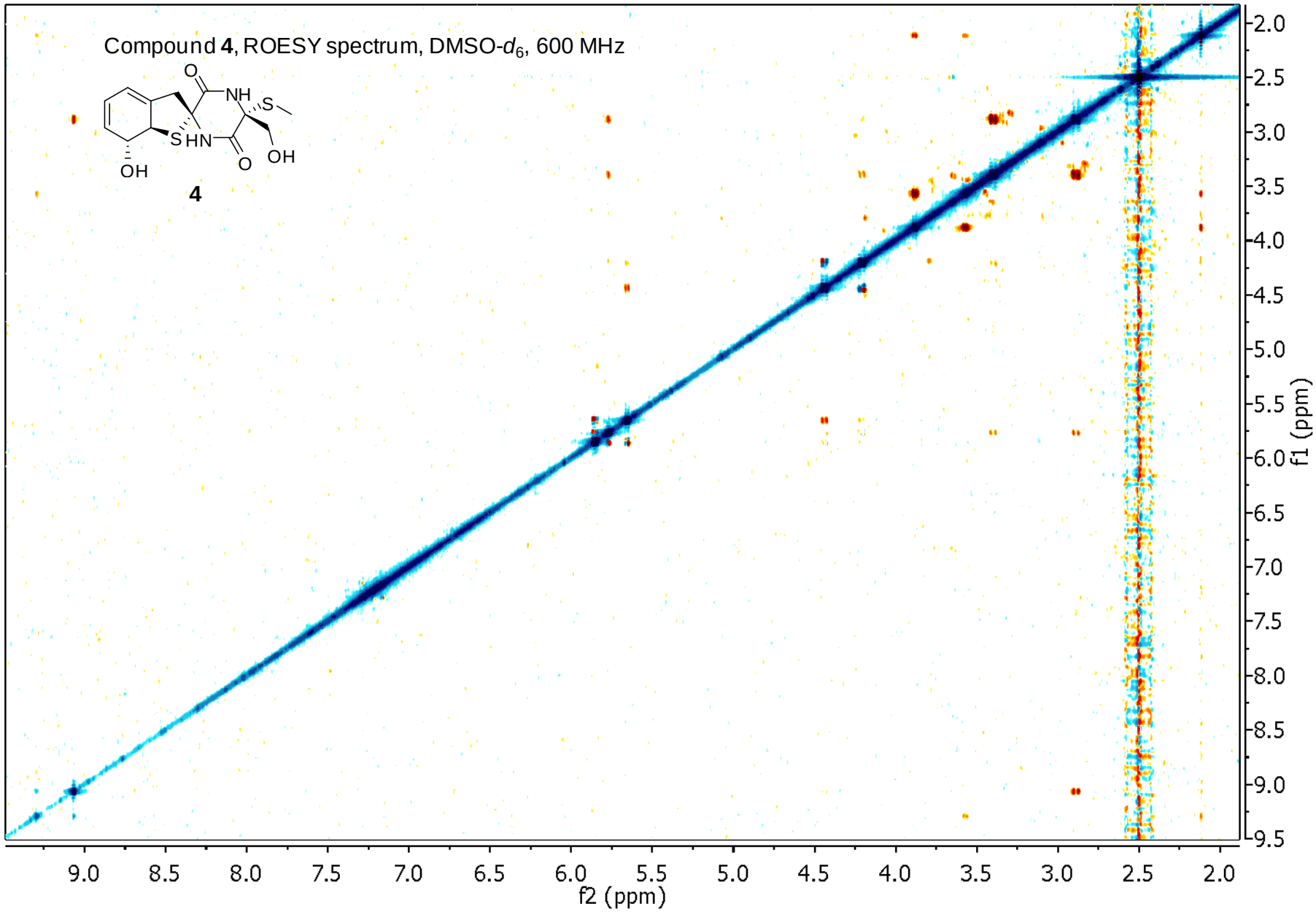
Compound 4, ROESY spectrum, DMSO-d6, 600 MHz
O
NH
S
S
HN
O
OH
OH
4
f2 (ppm)
f1 (ppm)
9.0
8.5
8.0
7.5
7.0
6.5
6.0
5.5
5.0
4.5
4.0
3.5
3.0
2.5
2.0
9.5

Compound **10**, ^{1}H NMR spectrum, acetonitrile-d_3, 500 MHz

10

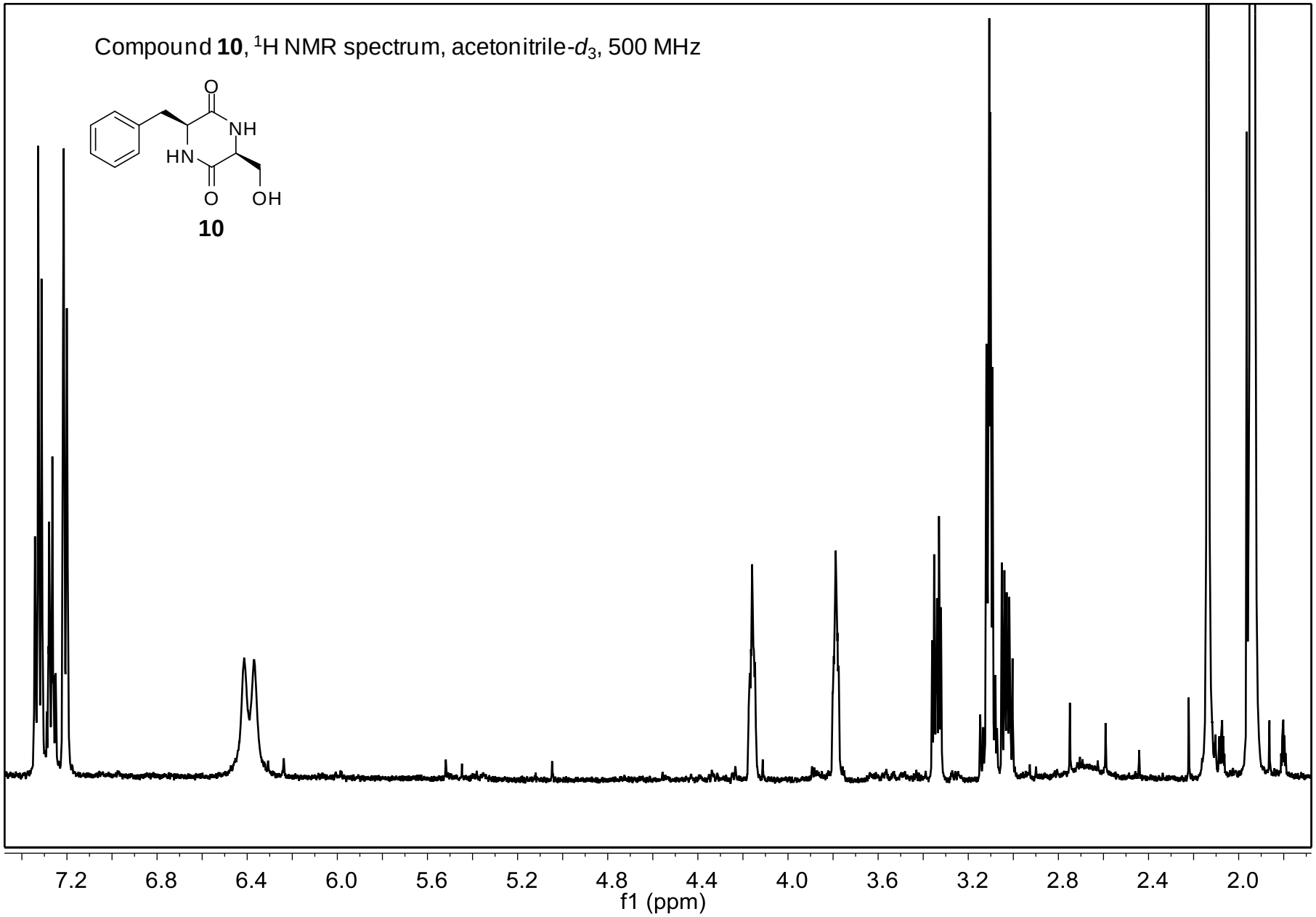

Compound **12**, ^{1}H NMR spectrum, acetonitrile-d_3, 600 MHz

12

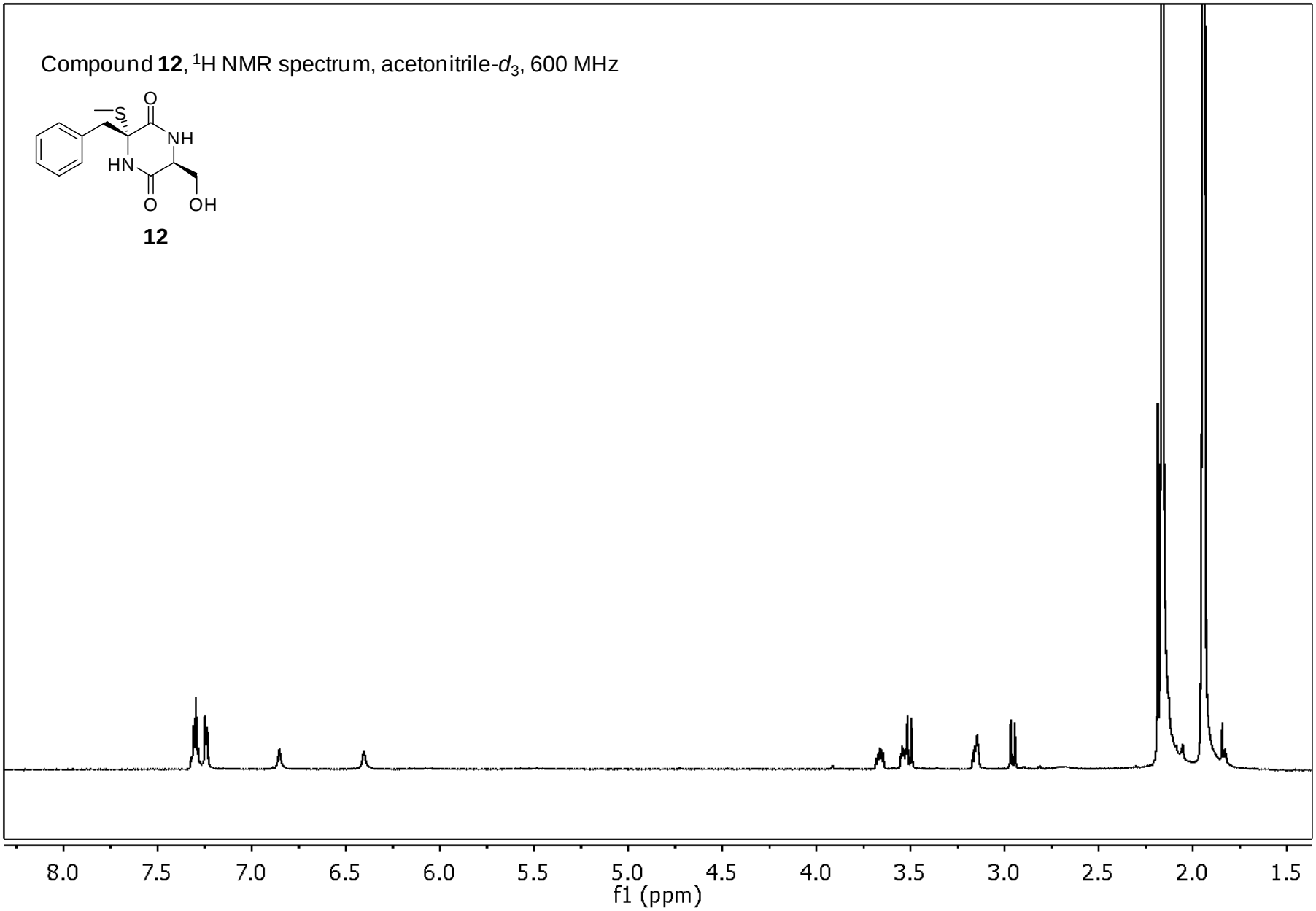

Compound **12**, ^{1}H NMR spectrum, acetonitrile-d_3, 600 MHz

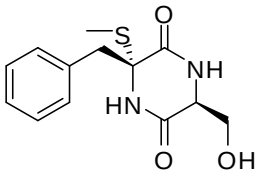

12

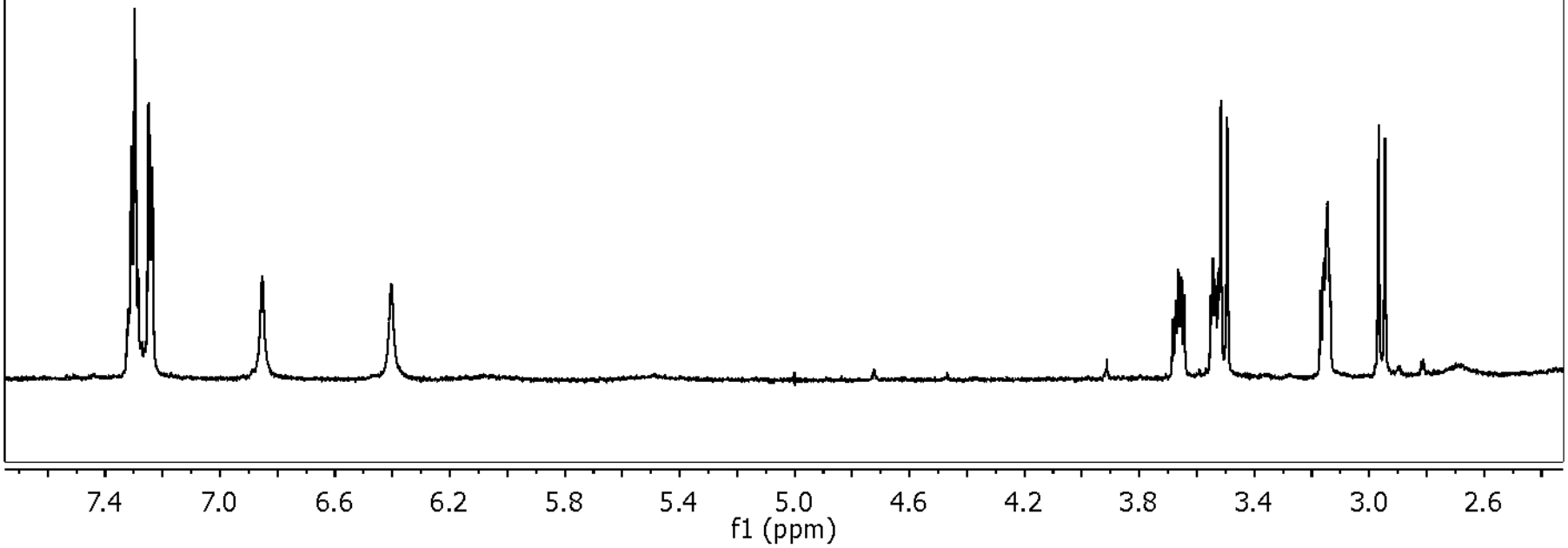

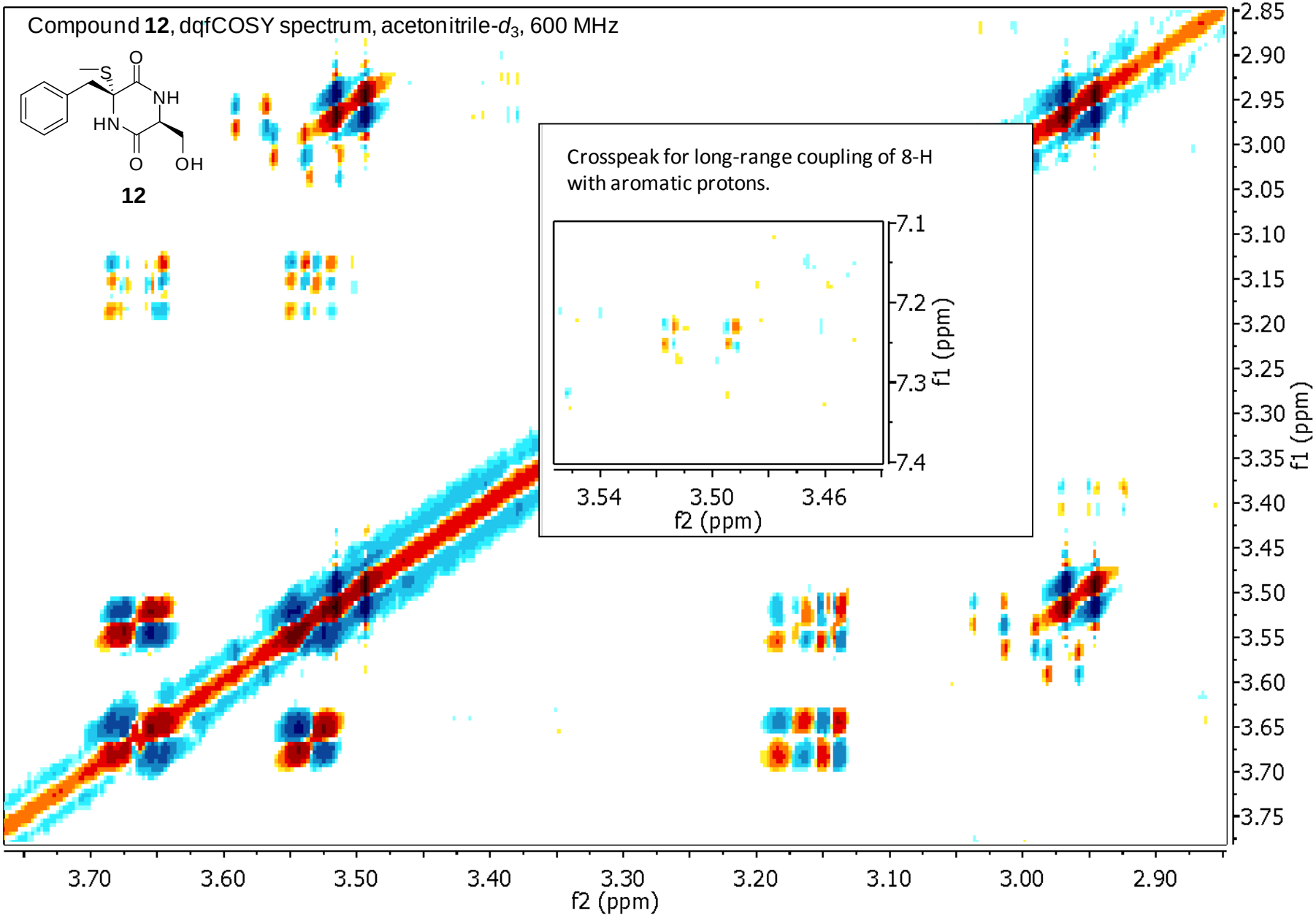
Compound 12, dqfCOSY spectrum, acetonitrile-d_3, 600 MHz
12
Crosspeak for long-range coupling of 8-H with aromatic protons.
f2 (ppm)
f1 (ppm)
3.70
3.60
3.50
3.40
3.30
3.20
3.10
3.00
2.90
2.85
2.90
2.95
3.00
3.05
3.10
3.15
3.20
3.25
3.30
3.35
3.40
3.45
3.50
3.55
3.60
3.65
3.70
3.75
3.54
3.50
3.46
7.1
7.2
7.3
7.4

Compound **12**, HMBC spectrum, acetonitrile-d_3, 600 MHz

12

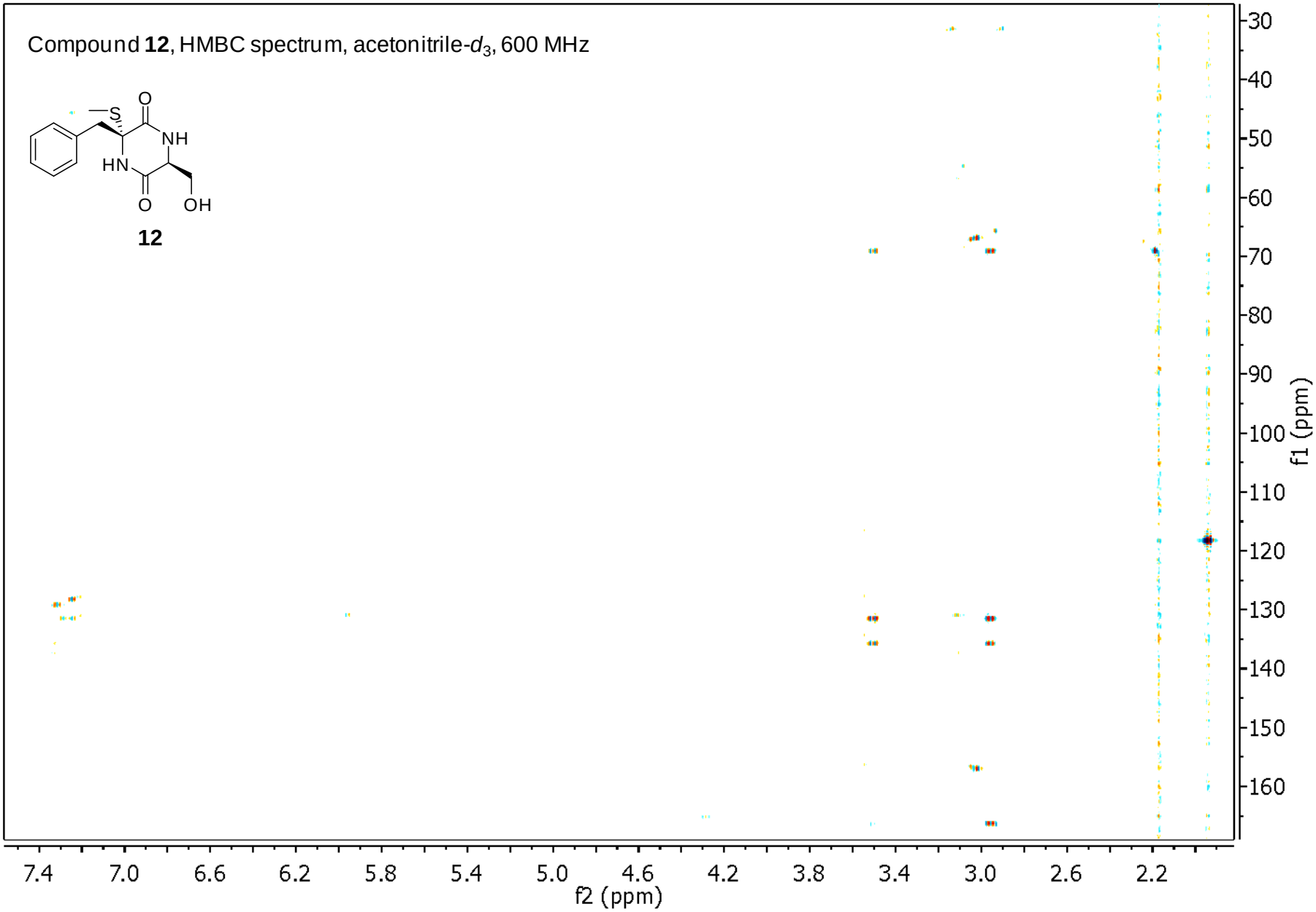

Compound **12**, HMBC spectrum, acetonitrile-d_3, 600 MHz

12

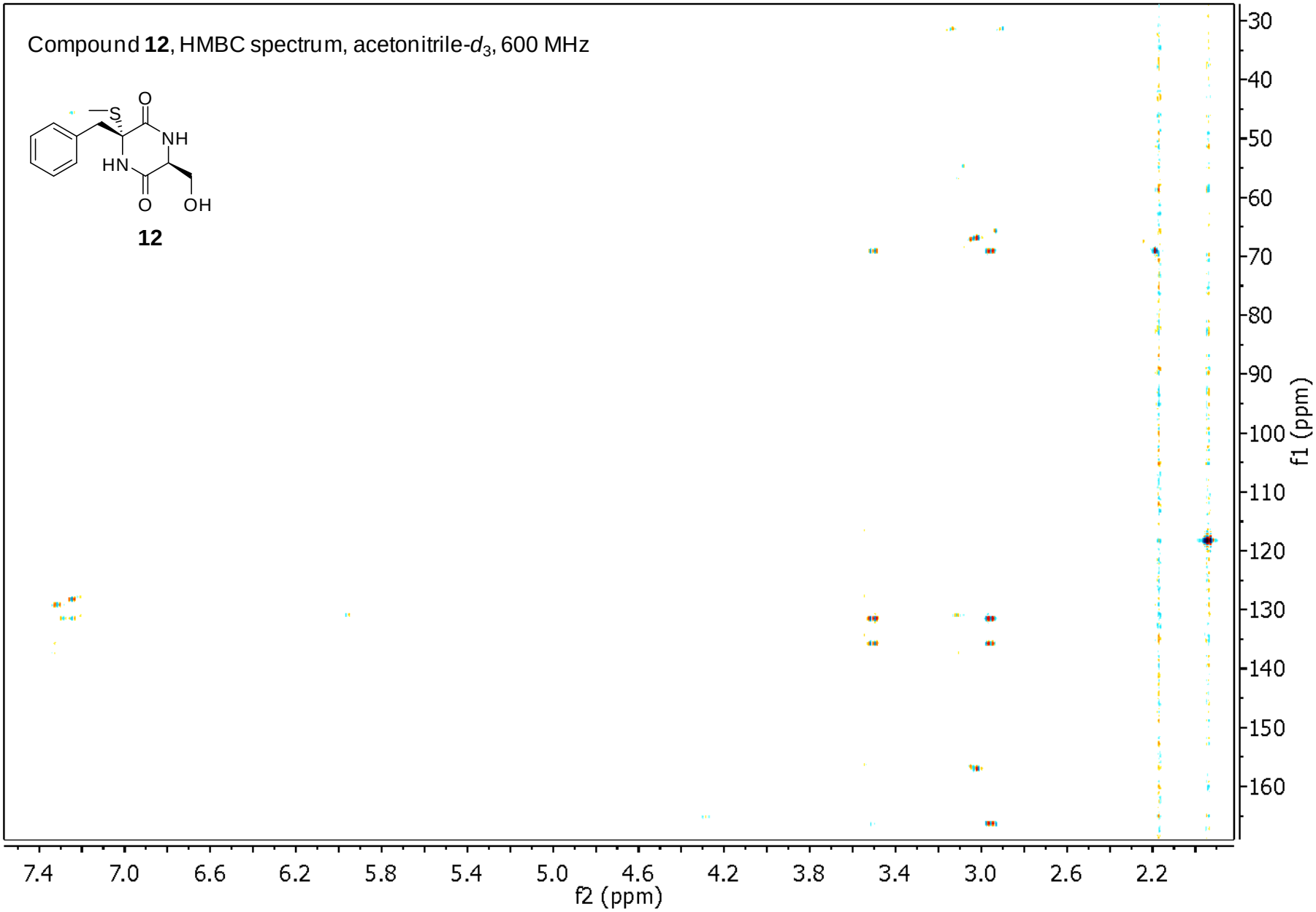

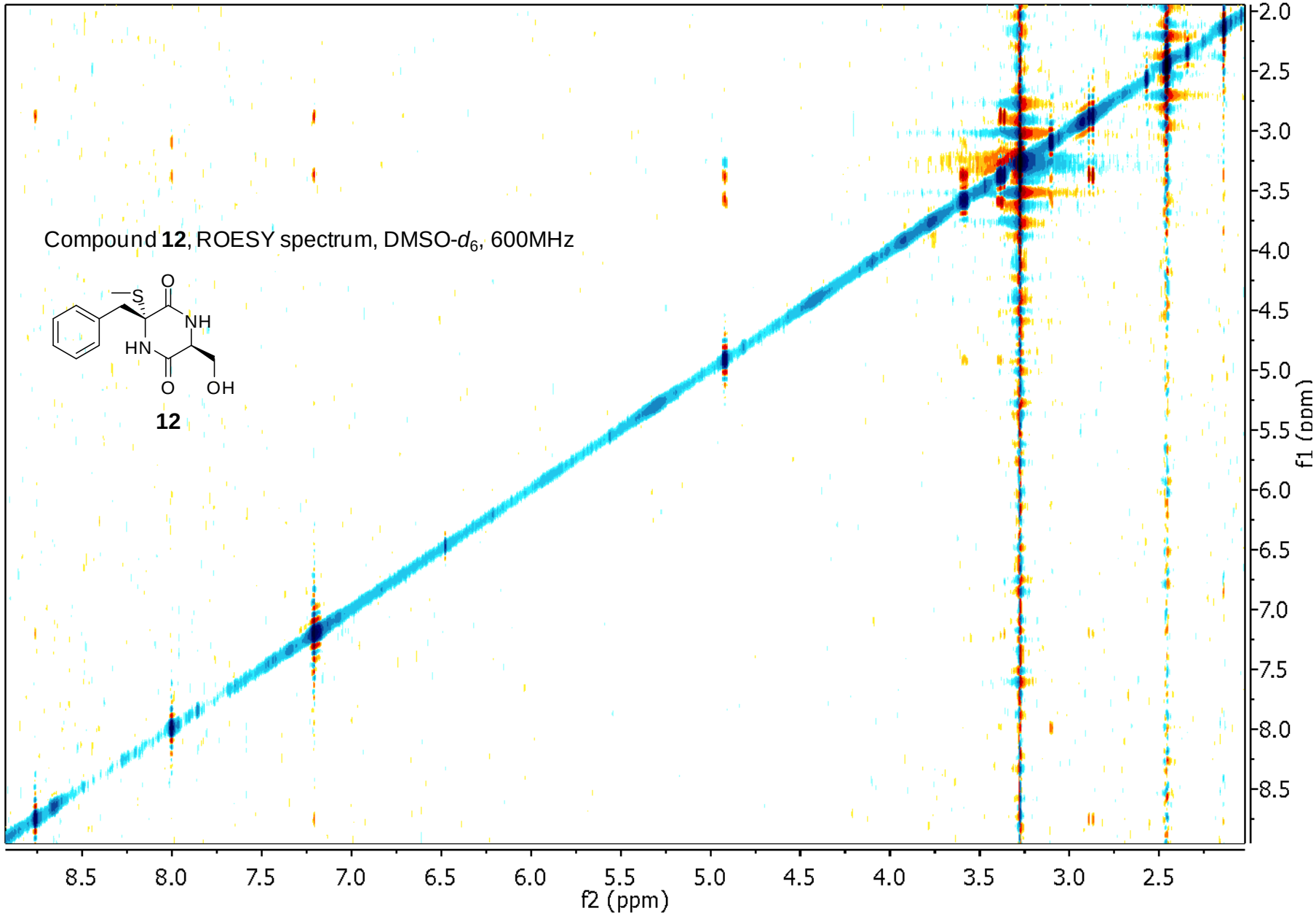
Compound **12**, ROESY spectrum, DMSO-d_6, 600MHz
S
O
NH
HN
O
OH
12
f2 (ppm)
f1 (ppm)
8.5
8.0
7.5
7.0
6.5
6.0
5.5
5.0
4.5
4.0
3.5
3.0
2.5
2.0
2.5
3.0
3.5
4.0
4.5
5.0
5.5
6.0
6.5
7.0
7.5
8.0
8.5

Compound **14a**, ^{1}H NMR spectrum, acetonitrile-d_3, 600 MHz

14a

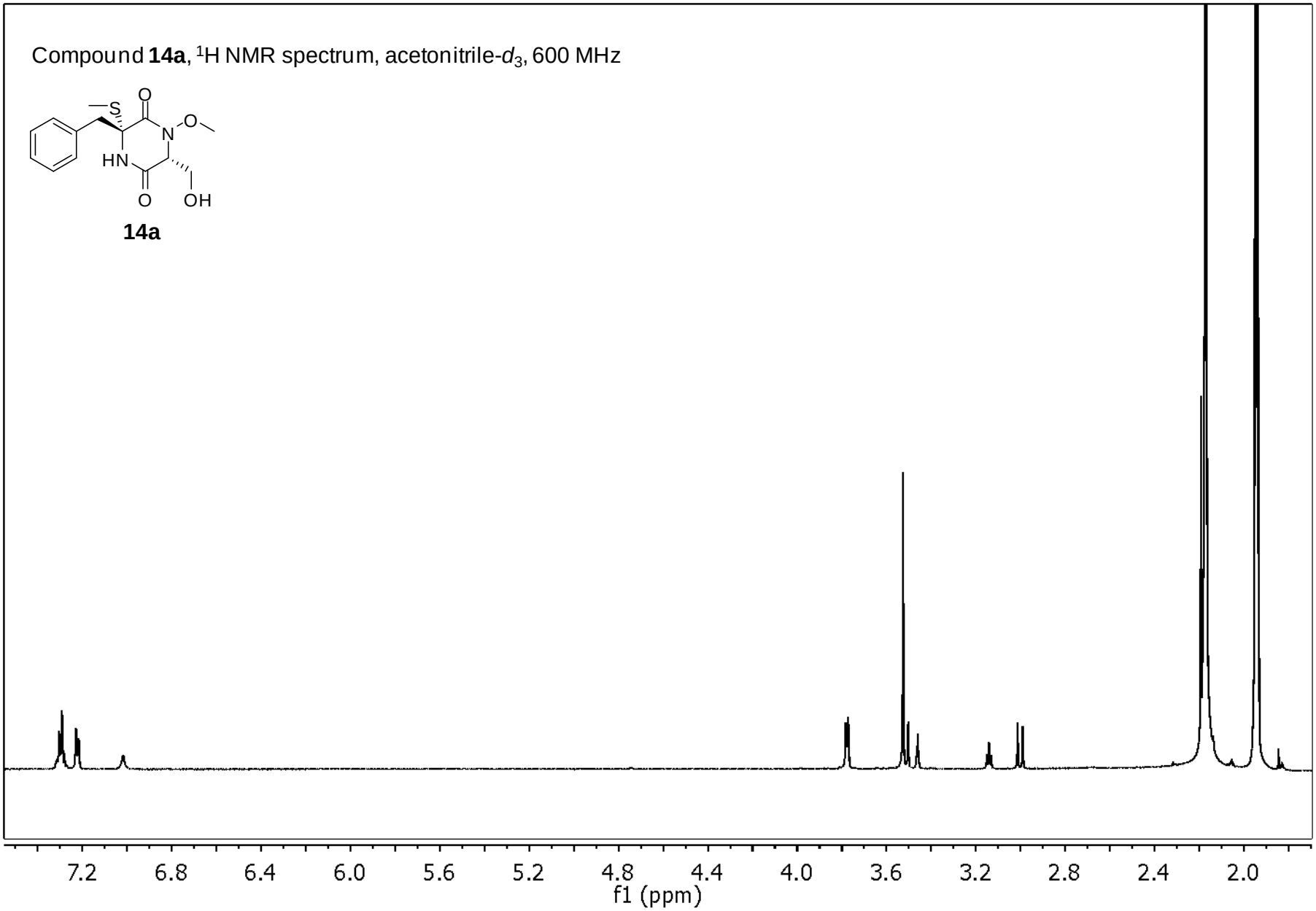

Compound **14a**, containing about 20% of its diastereomer **14b**,
dqfCOSY spectrum, acetonitrile-d_3, 600 MHz

14a

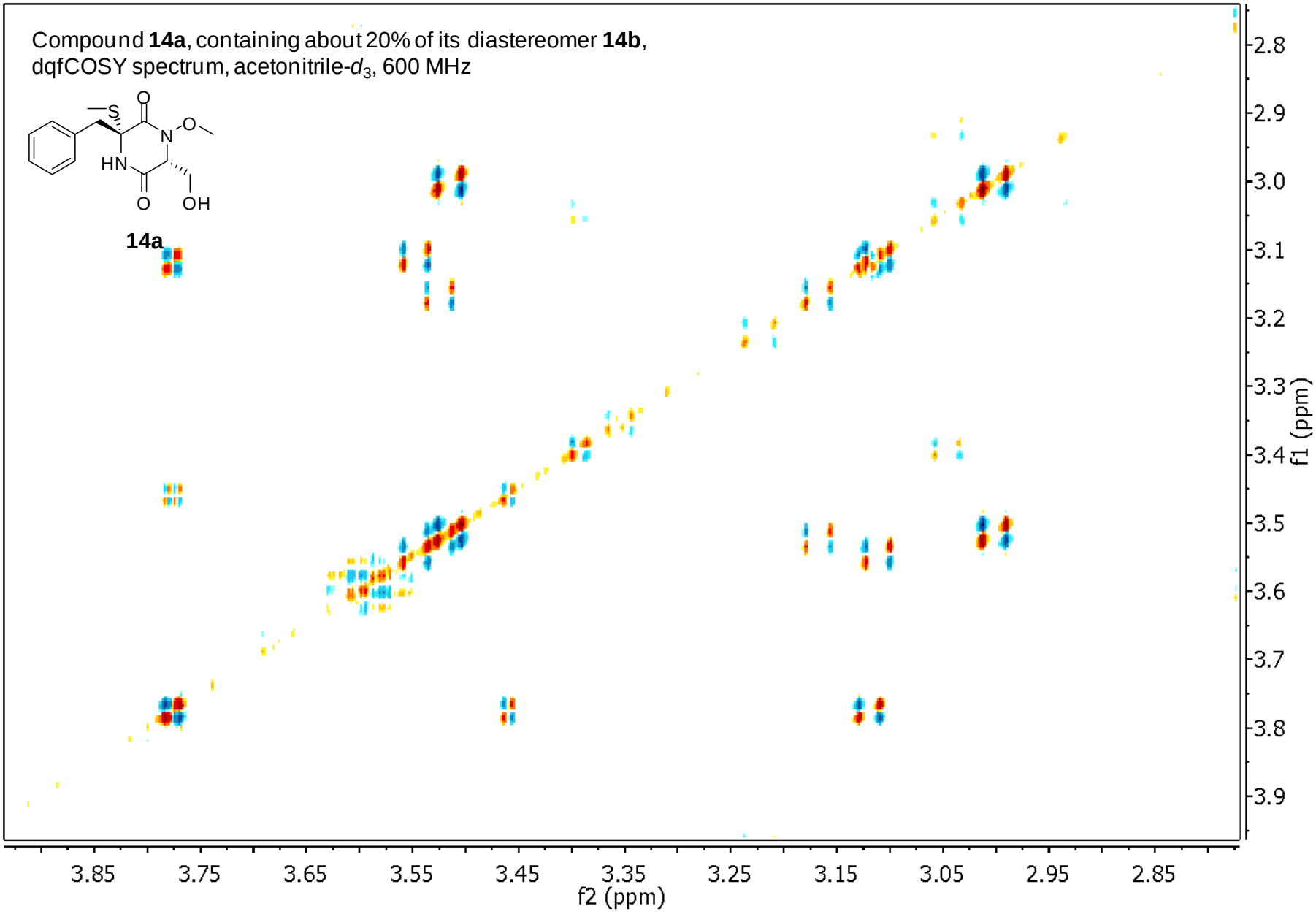

Compound **14a**, HSQC spectrum, acetonitrile-d_3, 600 MHz

14a

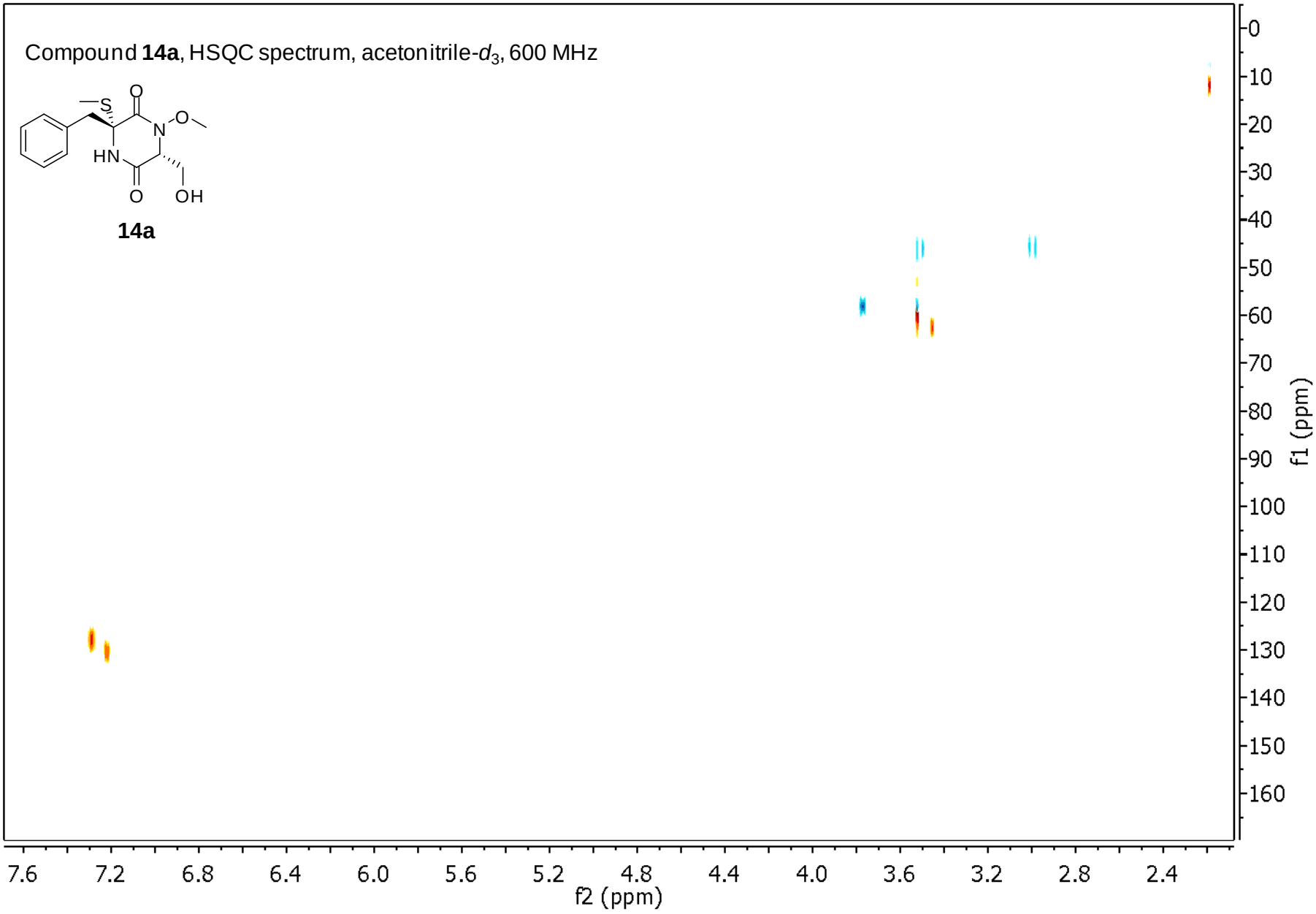

Compound **14a**, HMBC spectrum, acetonitrile-d_3, 600 MHz

14a

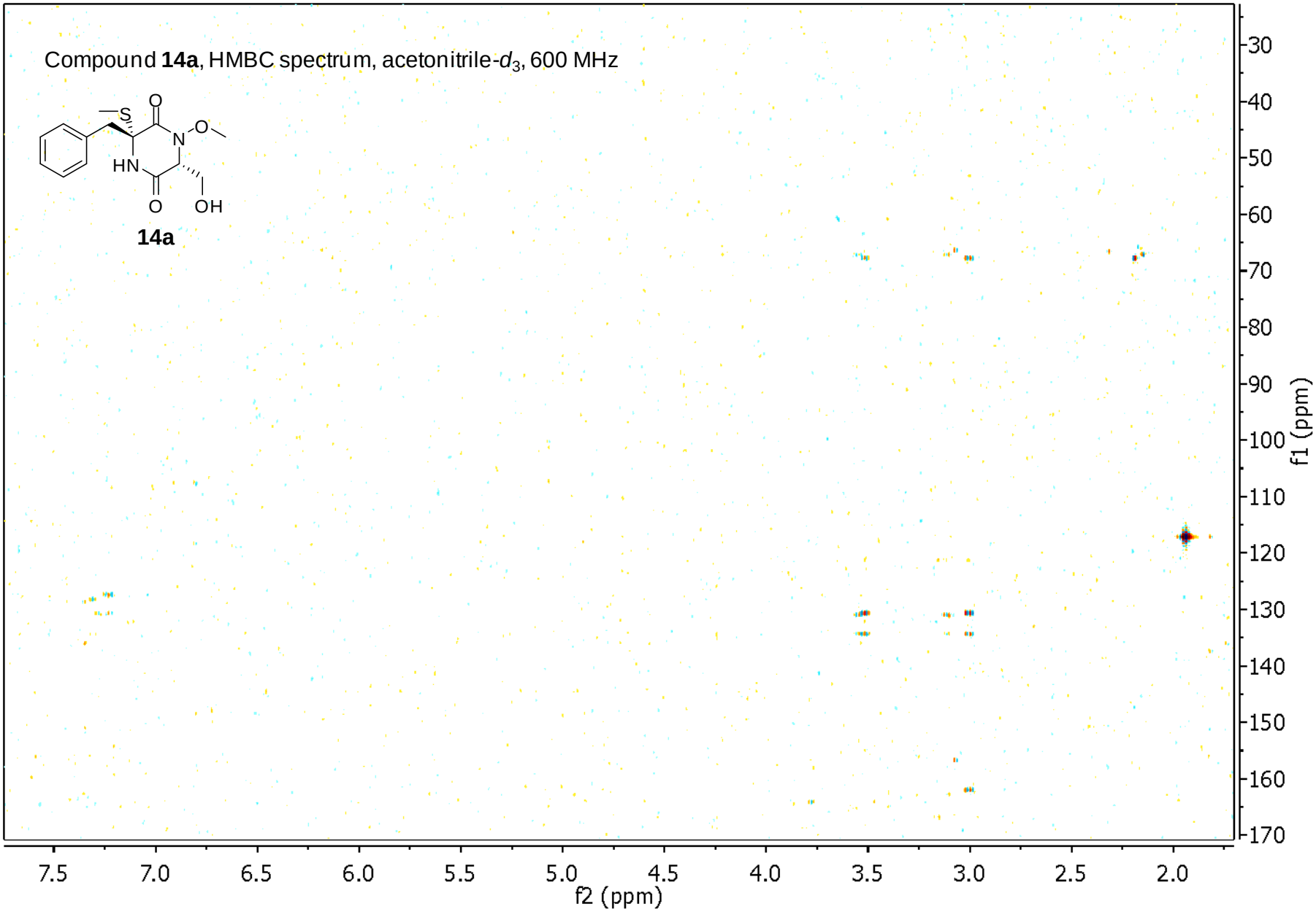

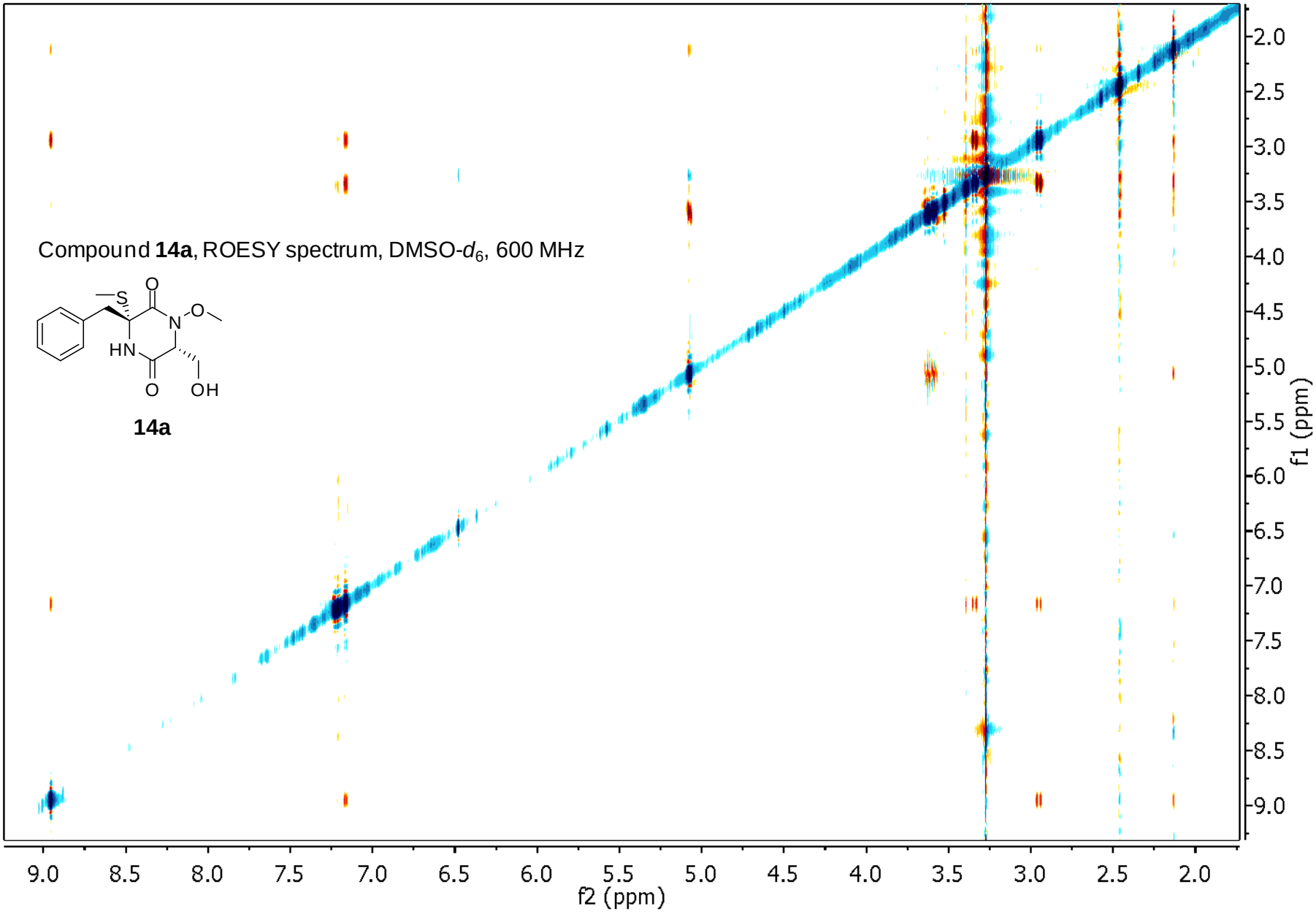
Compound **14a**, ROESY spectrum, DMSO-d_6, 600 MHz
S
O
N
O
HN
O
OH
14a
9.0
8.5
8.0
7.5
7.0
6.5
6.0
5.5
5.0
4.5
4.0
3.5
3.0
2.5
2.0
f2 (ppm)
2.0
2.5
3.0
3.5
4.0
4.5
5.0
5.5
6.0
6.5
7.0
7.5
8.0
8.5
9.0
f1 (ppm)

Compound **14a**, (^{1}H, ^{15}N)-HMBC spectrum, DMSO-d_6, 600 MHz

14a

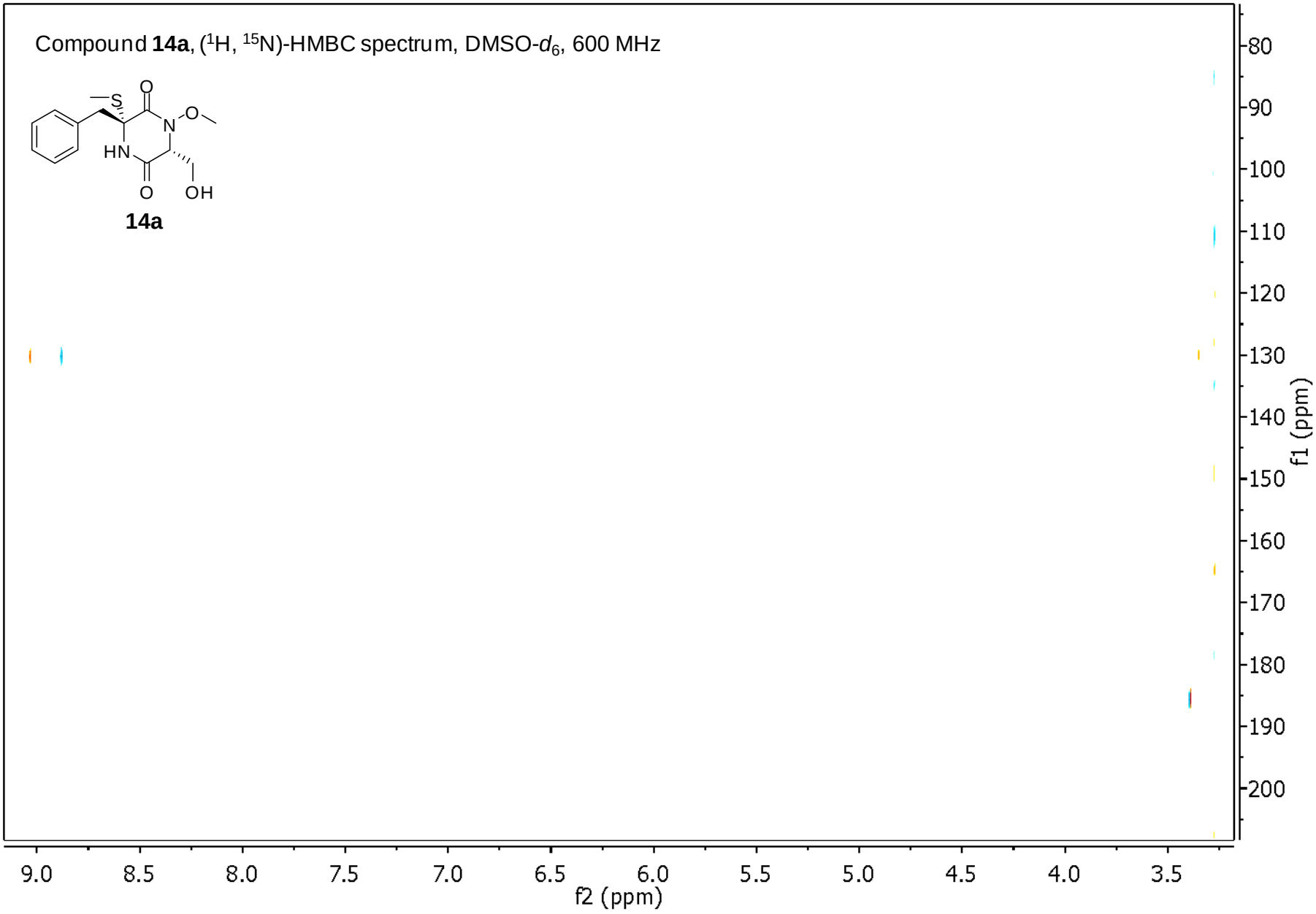

References

(1) Shimizu, K. and Keller, N. P. *Genetics*, **2001**, *157*, 591.

(2) Pungaliya, C.; Srinivasan, J.; Fox, B. W.; Malik, R. U.; Ludewig, A. H.; Sternberg, P. W.; Schroeder, F. C. *Proc. Natl. Acad. Sci. U.S.A.* **2009**, *106*, 7708.

(3) Schroeder, F. C.; Gibson, D. M.; Churchill, A. C.; Sojikul, P.; Wursthorn E. J.; Krasnoff, S. B.; Clardy, J. *Angew. Chem. Int. Ed. Engl.* **2007**, *46*, 901.

(4) Balibar, C. J. and Walsh, C. T. *Biochemistry*, **2006**, *45* 15029.